FACULDADE DE CIÊNCIAS E TECNOLOGIA
UNIVERSIDADE NOVA DE LISBOA

Departamento de Química

In vitro studies of Gum Arabic-coated Magnetic Nanoparticles with Mammalian Cell Cultures

Por
Ana Sofia Cardoso

Dissertação apresentada na Faculdade de Ciências e Tecnologia da Universidade Nova de Lisboa para obtenção do grau de Mestre em Biotecnologia

Orientadoras: Ana Cecília Afonso Roque
Ana Isabel Dias Bicho dos Santos

Lisboa
2008

Dissertação apresentada à Faculdade de Ciências e Tecnologia da Universidade Nova de Lisboa para cumprimento dos requisitos necessários à obtenção do grau de Mestre em Biotecnologia, realizada sob a orientação científica de Ana Cecília Afonso Roque, Professora Auxiliar, Faculdade de Ciências e Tecnologia da Universidade Nova de Lisboa e co-orientação de Ana Isabel Dias Bicho dos Santos, Investigadora, Faculdade de Ciências e Tecnologia da Universidade Nova de Lisboa.

Acknowledgements

I would like to acknowledge first and foremost my dear supervisors Prof. Ana Cecília Afonso Roque and Dr. Ana Isabel Dias Bicho dos Santos for all the endless support, guidance and especially for their friendship. To my fellow co-workers and also friends from the "NanoLab" and from the other laboratories, namely Ana Pina, Vera Castro, Dr. Abid Hussain, Telma Barroso, Íris Batalha, Ana Bárbara Santos, Ana Lanham, Nuno Costa, Ines Gomes, Pedro Quaresma, Tânia Carvalho, Leonor Morgado, Dr. Pedro Vidinha... I want to express my deepest gratitude for all the fruitful discussions and never ending support. I would also like to thank Dr. Paulo Lemos at the Bioengineering group (FCT-UNL) for all the help with the microscopy analysis, Dr. Pedro Baptista and Gonçalo Dória (CIGMH, FCT-UNL), for the help with the microplate reader, Dr. António Lopes at CoPos (ITQB - UNL) for allowing me to perform the DLS and Zeta Potential analysis, Eng. Isabel Nogueira (IST- UTL) for the TEM analysis and Prof. Isabel Fonseca (FCT-UNL) for the BET analysis. I would also like to acknowledge the help of Eng. Lúcia Pereira, Maria José Carapinha, Maria da Palma Afonso, Joaquina Lopes, Maria da Conceição Martins and Idalina Martins for all the help they provided throughout the work.

Last but certainly not the least, I would like to acknowledge all the support provided from my family and friends, especially my mother Manuela Cardoso and my grandmother Celeste Cristóvão for the endless love and support, and my friends Ricardo Araújo, Élio Soares and Ricardo Dias for always being there for me.

Index

Index of Figures

Index of Tables

Glossary

BET – Brunauer, Emmet and Teller

CHO – Hamster Chinese Ovary cells

DLS – Dynamic Light Scattering

FITC – Fluorescein isothiocyanate

FTIR – Fourier Transform Infrared Spectroscopy

GA – Gum Arabic

GA–FITC – Gum Arabic marked with Fluorescein isothiocyanate

HEK293 – Human Embryonic Kidney cells

MNPs – Iron Oxide Magnetic Nanoparticles

MNP – Magnetic Nanoparticles (uncoated)

MNP_{agg} – Magnetic Nanoparticles (uncoated) analyzed several days after synthesis

MNP_GA_{ADS} – Magnetic Nanoparticles with adsorbed Gum Arabic

MNP_GA_{APTS} – Magnetic Nanoparticles with covalently coupled Gum Arabic via Gum Arabic amine groups

MNP_GA_{EDC} – Magnetic Nanoparticles with covalently coupled Gum Arabic via Gum Arabic carboxyl groups

MNP_GA – Magnetic Nanoparticles co-precipitated with Gum Arabic

MNP_GA_{agg} – Magnetic Nanoparticles Co-precipitated with Gum Arabic analyzed 23 days after synthesis

$MNP\_GA\_GA_{ADS}$ – Magnetic Nanoparticles co-precipitated with Gum Arabic and with adsorbed Gum Arabic

MNP_GA_{ADS} – FITC – Magnetic Nanoparticles with adsorbed Gum Arabic marked with Fluorescein isothiocyanate

MNP_GA_{APTS} – FITC – Magnetic Nanoparticles with covalently coupled Gum Arabic via Gum Arabic amine groups marked with Fluorescein isothiocyanate

MNP_GA_{EDC} – FITC – Magnetic Nanoparticles with covalently coupled Gum Arabic via Gum Arabic carboxyl groups marked with Fluorescein isothiocyanate

$MNP\_GA\_GA_{ADS}$ – FITC – Magnetic Nanoparticles co-precipitated with Gum Arabic and with adsorbed Gum Arabic marked with Fluorescein isothiocyanate

TE671 – Human Caucasian Medulloblastoma cells

TEM – Transmission Electron Microscopy

Abstract

The aims of this work were the functionalization of magnetic nanoparticles (MNPs) with Gum Arabic (GA) and the study of the effect of these modified particles on the growth and survival of mammalian cell cultures. MNPs consisting of Fe_3O_4 were synthesized by the Massart Method and further functionalized with GA by adsorption and covalent coupling via GA amino or carboxylic acid groups. The GA adsorption and binding isotherms displayed a Langmuir type. The maximum of GA coated on MNPs followed the order $MNP\_GA_{APTS} < MNP\_GA\_GA_{ADS} < MNP\_GA_{ADS} < MNP\_GA_{EDC}$, where MNPs coated with GA via EDC activation gave the best result for coupling (2,80 g GA bound/g MNP for 2,62 mg/ml GA (eq.)). The particles were characterized by FTIR, BET, TEM and DLS, showing the greater dispersion and colloidal stability of particles in aqueous solution when GA is present. Cultures of mammalian cell lines (HEK293, CHO and TE671) were grown in the presence of uncoated and GA coated MNPs. Cellular viability was assessed for different incubation periods by means of the Trypan Blue exclusion test and by comparing cellular density with that of cells grown in the absence of particles. Different MNPs need different incubation periods to deposit at cellular surface, and the results vary with the cell type tested. With HEK293 cells, MNP_GA_{APTS} attach to the cell surface after only 30 minutes, while bare magnetite and MNP_GA_{EDC} have a greater effect on compromising cellular viability. On the other hand, MNP_GA_{ADS} needed longer incubation periods to attach to the cell surface and caused less cellular damage for identical incubation times with the other particles tested.

Resumo

Este trabalho teve como objectivos a funcionalização de nanopartículas magnéticas (NPMs) com Goma Arábica (GA) e o estudo do efeito das mesmas no crescimento e viabilidade de culturas de células de mamífero. NPMs constituídas por Fe_3O_4 foram sintetizadas pelo Método de Massart e funcionalizadas com GA por adsorção e ligação covalente através de grupos amina ou carboxilo da GA. As isotérmicas de adsorção de GA nas NPMs apresentaram o modelo de Langmuir. O máximo de GA ligada às NPMs seguiu a ordem $NPM\_GA_{APTS} < NPM\_GA\_GA_{ADS} < NPM\_GA_{ADS} < NPM\_GA_{EDC}$, obtendo-se os melhores resultados para a ligação das NPMs à GA através da activação com EDC (2,80g GA ligada/g NPM para 2,62 mg/ml GA (eq.)). As partículas foram caracterizadas por FTIR, BET, TEM e DLS. Verificou-se que a presença de GA permite uma maior dispersão e estabilidade coloidal das partículas em solução aquosa. Culturas de linhas celulares de mamíferos (HEK293, CHO e TE671) foram crescidas na presença de NPMs com e sem GA. A viabilidade celular foi verificada para diferentes tempos de incubação através do teste de exclusão com Azul de Trypan e por comparação com a densidade celular de células crescidas na ausência de partículas. Diferentes NPMs necessitam de diferentes tempos de incubação para se depositarem à superfície celular, e os resultados variam com o tipo de célula testado. Com as células HEK293, as NPM_GA_{APTS} ligam-se à superfície celular logo após 30 minutos, enquanto que as partículas de magnetite (NPM) e as NPM_GA_{EDC} comprometeram mais fortemente a viabilidade celular. Por outro lado, NPM_GA_{ADS} necessitaram de maiores períodos de incubação que as outras partículas testadas, para se ligarem à superfície celular, e causaram menores danos para os mesmos tempos de incubação.

Chapter 1 – Literature Review

The term "nanotechnology" was firstly used by Professor Norio Taniguchi in 1974: "'Nano-technology mainly consists of the processing of, separation, consolidation, and deformation of materials by one atom or by one molecule [1]. Although there is not a uniformly agreed definition of nanotechnology (derived from the Greek word nano meaning dwarf), the widely accepted National Nanotechnology Initiative (NNI) definition states: "[Nanotechnology refers to] the understanding and control of matter at dimensions of roughly 1 to 100 nanometers, where unique phenomena enable novel applications [2].

Nanoparticles are structures between 1 and 100 nanometers, which may be synthetic (e.g. catalysts and probes) or naturally occurring (e.g. colloids, aerosols). These particles may be subclassified, as being organic (carbon containing) or inorganic, and relatively to their structure, as sphere, tube, colloid, quantum dot, fiber, rod, crystal, fullerene or other. Nanoparticles may also contain oxides, metals, salts, polymer and aerosol that are critical to function. Colloids, aerosols, and even viruses are examples of naturally occurring organic nanoparticles, synthetic nanoparticles include catalysts and probes [3, 4]. Nanoparticles are one of the important building blocks in the fabrication of nanostructured materials and devices with adjustable physical and chemical properties. As intermediates between the molecular and the solid states, inorganic nanoparticles combine chemical accessibility in solution with physical properties of the bulk phase, displaying unique electrical, optical, mechanical and magnetic properties.
Nanotechnology can be roughly divided into categories that include nanobiotechnology, biological micro-electromechanical systems, microfluidics, biosensors, microarrays [5] , and tissue microengineering [6].

1.1. Magnetic Nanoparticles

Different kinds of noble metals, e.g. Au and Ag, and magnetic nanoparticles, e.g. γ-Fe_2O_3, Fe_3O_4 and FePt, have been synthesized for different applications [7-17]. Iron oxide nanoparticles (Fe_3O_4) have been applied in *in vitro* diagnostics for nearly 40 years. Iron oxide/magnetite particles (Fe_3O_4) or maghemite (γ -Fe_2O_3) are by far the

most commonly studied and employed for biomedical applications (5-20 nm in diameter) [18, 19]. Several applications of magnetic iron oxide nanoparticles are summarized in Table 1-1. Magnetite is considered to be a very promising candidate because its biocompatibility has been already proven [18, 20, 21].

Table 1-1 Potential applications for magnetic iron oxide (Fe_3O_4) nanoparticles

	MNP Type	Applications	References
Medical	50 – 100 nm sized Fe_3O_4 nanoparticles	Drug targeting and delivery - Local chemotherapy	[7, 10-13, 22]
	MNPs with ligands attached	Recognition and attachment to damaged or diseased tissue followed by release therapeutic compound e.g. Buckyball-based treatment for AIDS	
	Fe_3O_4 nanoparticles	Hyperthermia treatments against cancer	[17]
		Tissue repair and engineering	[23]
Diagnostic	Fe_3O_4 nanoparticles	Electrochemical immunoassay	[24]
		Magnetic imaging applications (MRI)	[3, 10, 12]
		Cell labelling (*in vivo*)	[25]
		Separation/selection, Magnetofection Magnetorelaxometry and Magnetic ELISA	[18, 26-28]
		Detection of early stage diseases such as cancer to allow early treatment	[29]
		Portable diagnostic labs for pharmaceutical chemical industry or disease prevention and control	[29]
Bioremediation / Bioseparation	Fe_3O_4 nanoparticles treated with Gum Arabic	Environmental contaminant remediation - removing copper ions from aqueous solutions	[30]
	Iron/iron oxide nanoparticles	Removal of trace catalyst impurities (Co^{2+}, Ni^{2+}, Rh^{x+}, Pd^{2+}, Ag^{+} and Pt^{4+}) from coordinating environments.	[31]
Other Biotechnological applications	Modified Fe_3O_4 nanoparticles	Biomagnetic separation and purification	[24, 32-34]
		Biomolecules immobilization	[35, 36]
		Catalysis	[9]

In the absence of any surface coating, magnetic iron oxide particles have hydrophobic surfaces. Nevertheless, due to anisotropic dipolar attraction, arising out of large surface area to volume ratio, unmodified magnetic nanoparticles of iron oxide tend to aggregate into large clusters that are non-biocompatible [37].

1.2. Synthesis and modification of Iron Oxide Magnetic Nanoparticles

In the present work iron oxide (Fe_3O_4) magnetic nanoparticles synthesized by the Massart's Method [38] were used.

Nanoparticles may be synthesized by gas phase deposition, electron beam lithography, thermal decomposition of iron pentacarbonyl and sonochemical decomposition of Iron carbonyl [19, 21]. Nanoparticles may also be prepared by partial oxidation of aqueous ferrous hydroxide gel [39], sol-gel preparation or polymer matrix-mediated synthesis [19]. The wet chemical routes to prepare magnetic nanoparticles such as reduction of Iron Salts and Oxides ("arrested precipitation") are considered to be simpler and efficient, controlling size, composition and sometimes the shape of the nanoparticles. Magnetite particles can be prepared by alkalinizing stoichiometric mixtures of ferrous and ferric ions with aqueous NH_3 in aqueous solutions or in microemulsions at room temperature. The most used method for the synthesis of iron oxides (Fe_3O_4 or γ-Fe_2O_3) is the co-precipitation of Fe^{2+} and Fe^{3+} aqueous salt solutions by addition of a base, conventionally, magnetite is prepared by adding a base to an aqueous mixture of Fe^{2+} and Fe^{3+} chloride at a 1:2 molar ratio (Massart's Method) [38]. The control of size, shape and composition of nanoparticles depends on the Fe^{2+} and Fe^{3+} ratio, the type of salts used (e.g. chlorides, sulphates, nitrate and perchlorates), pH and ionic strength of the media. Removing the oxygen from the environment, not only protects critical oxidation of the magnetite but also reduces the particle size [19].

The nanoparticles surface may be modified in order to increase stabilization against agglomeration (due to hydrophobic interactions between the particles), to render them compatible with another phase, to enable their self-organization or to make the nanoparticles biocompatible [40]. Nanoparticles may be functionalized by inorganic and also organic groups: simple organic groups have the ability to prevent nanoparticles from agglomerating and functional organic groups on the particle surface may allow deliberate interaction of the nanoparticles with molecules, other particles, surfaces, or solids [40]. Iron oxide nanoparticles, may be modified by thiols, carboxylic acids, amines, and specially by phosphonates or silanes [36, 40-43]. For biological applications, the particles must have combined properties of biocompatibility, interactive functions at the surface and high magnetic saturation. During nanoparticle synthesis, a surfactant [44-47] or a polymer [48] may be added in order to prevent aggregation of nanoscale particulate and increase biocompatibility [18]. Nanoparticles may also be coated with a biocompatible polymer after the synthesis. Steric stabilization can be induced by surface attachment of various natural or synthetic polymers, either by adsorption, hydrophobic insertion, electrostatic binding, or, preferably, by grafting via

covalent bond. Nonionic, water compatible, flexible and well-hydrated polymers are preferred [49]. Several types of coatings have been studied for the surface modification of nanoparticles, such as natural and synthetic polymers [7]. The table summarizes some of the different coatings used for nanoparticle modification [7, 25].

Table 1-2 Different compounds which can be used for nanoparticle coating (adapted from [7]).

Compounds		References
NATURAL	Albumin	[15, 50]
	Alginate	[51]
	Chitosan	[48, 52-55]
	Dextran Dextrin	[48, 56] [15, 57]
	Fatty acids	[58]
	Gelatin	[14]
	Gum Arabic	[48, 58-62]
	Polypeptides	[63, 64]
	Phosphorylcholine	[65]
	Silica	[51, 54, 66]
	Oleic acid	[55, 67]
	Oleylamine	[59]
SYNTHETIC	Polyacrylic acid	[67]
	Polyethylene glycol (PEG)	[7, 16, 49, 56, 59, 68]
	Poly (D, L-lactide)	[50]
	Poly(*N*-isopropylacrylamide) (PolyNIPAAM)	[69]
	Polyvinyl alcohol (PVA)	[70]
	Polyvinylpyrrolidone (PVP)	[71]

Gum Arabic

Gum Arabic (GA), the technical name for Acacia Senegal Gum, is the dried gummy exudates from the stems and branches of *Acacia senegal* (Linné) Wildenow or of other related African species of Acacia (Family Leguminosae). This naturally occurring compound with reported molecular weights of approximately 850,000 and 240,000, is made up of a high molecular weight glycoprotein containing 90% carbohydrate and a protein content ranging from approximately 1.5% to 3% for samples from various producing areas, and a lower molecular weight heterogeneous polysaccharide. GA has also been described as a complex mixture of calcium, magnesium, and potassium salts of arabic acid. GA is composed of D-galactose, L-rhamnose, L-arabinose, and D-glucuronic acid residues in an arrangement of a main chain of galactosyl units joined by

β-D-(1→3) linkages and side chains or branched oligosaccharides linked to the main chain by β-D-(1→6) linkages. The oligosaccharides may contain terminal rhamnosyl units linked (1→3) or terminal arabinofuranosyl units linked (1→4) to internal galactosyl or glucuronosyl units [72]. The proposed "waddle blossom" structure for GA with a number of polysaccharide units linked to a common polypeptide chain is presented in the figure:

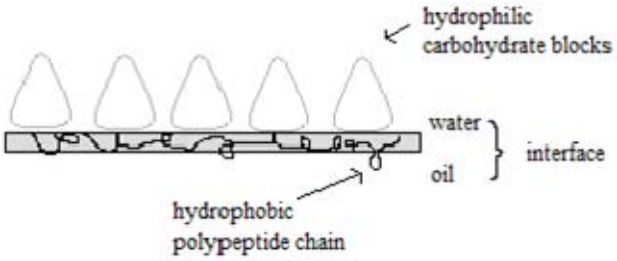

Figure 1-1 Proposed structure for GA (after Islam et al [73]).

GA is a substance that is generally recognized as safe (GRAS) for direct addition to human food and cosmetic formulations. It has been used in various industries as an emulsifier and stabilizer for oils and flavourings [73-76]. Is negative in several genotoxicity assays, is not a reproductive or developmental toxin, and is not carcinogenic when given intraperitoneally or orally. Clinical testing indicated some evidence of skin sensitization with GA [72]. Pharmacologically, GA has been claimed to act as an anti-oxidant, to protect against experimental hepatic-, renal- and cardiac toxicities in rats, and to alleviate the adverse effects of chronic renal failure in humans. Reports on the effects of GA on lipid metabolism in humans and rats are at variance, but mostly suggest that GA ingestion can reduce plasma cholesterol concentrations in rats. GA has proabsorptive properties and can be used in diarrhoea. GA enhances dental remineralization, and has some antimicrobial activity, suggesting a possible use in dentistry. No significant adverse or toxic actions have been associated with the use of GA [77].

This remarkable and complex material has displayed the ability to sustain colloidal stability for carbon nanotubes in aqueous solutions due to unspecific physical adsorption [61], acts as a steric stabilizer in the preparation of colloidal copper particles [62] and in the preparation of biocompatible quantum dot nanocolloids [78].

Due to the stabilization ability and the biocompatibility of Gum Arabic, this polymer has been tested by several groups for the surface modification of magnetic nanoparticles

for very different applications (as it can be seen from Table 1-1 and Table 1-2). Wilson et al (2008) [59], used Gum Arabic for the surface modification of magnetic nanoparticles, in order to stabilize the colloidal suspension of magnetic nanoparticles to be used in interaction studies with L929 fibroblast cells. In the same study magnetic nanoparticle co-precipitation with oleylamine was also tested. Banerjee et al (2007) [60] grafted Glucose into Gum Arabic modified magnetic nanoparticles so as to study the specific interaction with concanavalin A. In 2007 and 2008, the same group [79, 80] fabricated a novel magnetic nanocarrier for targeted anticancer drug delivery by conjugating cyclodextrin onto Gum Arabic modified magnetic nanoparticles using hexamethylene diisocyanate as a linker. Jayakrishnan et al, in 2007 [81], prepared a self-gelling primaquine-(periodate-oxidized)Gum Arabic conjugate for injectable controlled delivery system for primaquine in anti malaria and antileishmanial therapies, and also in 2007, the same group synthesized and evaluated ampicillin-conjugated (periodate-oxidized) Gum Arabic microspheres for sustained release [82].

1.3. Interaction of Magnetic Iron Oxide Nanoparticles and Cells

All nanoparticles synthesized and surface modified with the proper coating materials and developed for biomedical applications, need to be further tested in contact with cells – *in vitro* studies to ascertain the influence on cellular growth and viability. Table 1-3 summarizes the examples of such studies.

Studies have also been performed on cell interactions with Gum Arabic conjugates: Jayakrishnan et al [81], in 2007, prepared a self-gelling primaquine-(periodate-oxidized)Gum Arabic conjugate for injectable controlled delivery system for primaquine in anti malaria and antileishmanial therapies. Cytotoxicity evaluation using MTT assay against L929 mouse fibroblasts showed that oxidized gum Arabic having a degree of oxidation of 50% was only very mildly cytotoxic at a concentration of 0,025 g/ml. Also in 2007, the same group synthesized and evaluated ampicillin-conjugated (periodate-oxidized)Gum Arabic microspheres for sustained release [82].

Table 1-3 Interaction studies of magnetic iron oxide nanoparticles and cells.

Nanoparticle Coating	Cell type	Application	Reference
-	Lung epithelium cells	Study of pulmonary response to MNPs	[83]
2-aminoethyl-phosphonic acid/Folic acid	Human cervix adenocarcinoma HeLa and human osteosarcoma, MG-63 cell lines	Cancer-specific targeting	[37]
(5-hydroxy-5,5 -bis-(phosphono) pentanoic acid	MDA-MB-231 and MDA-MB-435 breast cancer cells	Diagnostics and therapy	[84]
Ceruloplasmin and lactoferrin	Human dermal fibroblasts	Targeting cell surface receptors	[85]
Chitosan	Human dermal fibroblasts	Cell invasion in tissue engineering	[52]
Citrate anions	Mammalian cells: *Immune cells*: raw macrophages (mouse); hybridomas (mouse); dendritic cells (human); OT-1 lymphocytes (mouse); EL4-B lymphocytes (human). *Therapeutic adult cells:* hepatocytes (mouse); gingival fibroblasts (human); smooth muscle cells (rat). *Therapeutic stem cells or progenitor cells:* myogenic precursor cells (pig); endothelial progenitor cells (human). *Tumor cells:* HeLa ovarian carcinoma (human); PC3 prostatic carcinoma (human); HuH7 hepatic carcinoma (human).	Cell labeling	[86]
Dextran	Human natural killer (NK) T cells	Cell labeling	[25]
Dextran	Adherent human prostate cells (DU-145) and murine suspension lymphoma cells	Cancer therapy, blood purification, lymph node imaging, hyperthermia	[87]
Dimercaptosuccinic acid	Human monocytic cell line, U937	MRI	[88]
Gum Arabic and Oleylamine	L929 fibroblasts	Cell targeting	[59]
Polyethylene glycol (PEG) and folic acid	Mouse macrophage (RAW 264.7) and human breast cells (BT20)	Improve cell internalization and target cancer cells	[56]
Polyethylene glycol (PEG)	Human dermal fibroblasts	Drug delivery and targeting	[16]
Silica/Polyethyleneimine (PEI)	HEK293 T cells	DNA-binding and transfection	[89]
Transferrin	Human dermal fibroblasts	Drug targeting	[90]

Earlier this year, Wilson et al. (2008) [59], synthesized MNPs in oleylamine (OLA) and Gum Arabic presence in order to study the influence of surface modification on MNP characteristics and cellular level bioactivity. The interactions studies were performed with L929 fibroblasts and three types of MNPs (bare magnetite, Oleylamine (OLA)-coated MNPs and Gum Arabic (GA)-coated MNPs).

1.4. Aims of the work

The main goals of this project were the functionalization of magnetic nanoparticles (MNPs) with a biocompatible polymer known as Gum Arabic (GA) and the study of the effect of these modified particles on the growth and survival of mammalian cell cultures.

In order to achieve these goals several studies were performed: optimization of magnetic nanoparticle synthesis by the Massart Method, optimization of Gum Arabic quantification in aqueous solutions using the microplate BCA Assay, study and optimization of adsorption and covalent coupling of Gum Arabic to functionalized magnetic nanoparticles via GA amino or carboxylic acid groups, MNP characterization by FTIR, BET, TEM and DLS, displacement studies of Gum Arabic adsorbed and covalently coupled onto magnetic nanoparticles in phosphate ion presence and the *In vitro* study of functionalized nanoparticles interactions with cells – cellular viability and growth studies. Cellular viability was assessed for different incubation periods by means of the Trypan Blue exclusion test and by comparing cellular density with that of cells grown in the absence of particles.

Chapter 2 – Synthesis of Magnetic Nanoparticles

2.1. Introduction

Magnetic nanoparticles (MNPs) are particles composed of a magnetite Fe_3O_4 or maghemite (γ- Fe_2O_3) core, with sizes ranging from 5 – 100 nm. Applications of MNPs cross through industry, biomedicine and other biologically related fields [17, 23]. Powder or composite MNPs are being studied for *in vivo* and *in vitro* applications. The former involves applications in medical diagnostic (magnetic resonance imaging (MRI) [11, 12, 17]) and in therapeutics (hyperthermia treatments against cancer [17], drug targeting and drug delivery [11-13]); the latter involves cellular therapy, bioseparation processes, tissue repair, magnetofection and gene therapy [26, 27], magnetorelaxometry and magnetic ELISA [28]. For these purposes, MNPs must have combined properties of high magnetic saturation, biocompatibility and interactive functions at the surface. MNPs surface modification can be performed by the creation of a few atomic layers of an organic polymer, an inorganic metal (e.g. gold), or oxide surfaces (e.g. silica or alumina), suitable for further functionalization with various bioactive molecules [19]. Several surface modification studies have been performed in iron oxide nanoparticles, including the use of surfactants for control of nanoparticle size by reduction of agglomerates formed during and after MNP synthesis [91, 92]. MNPs tend to agglomerate during synthesis in order to reduce surface energy, a process facilitated by strong magnetic dipole-dipole attraction [62]. Tetramethylammonium hydroxide (TMA) has been also used efficiently in redispersing nanoparticle agglomerates [92] but it is not biocompatible due to its high alkalinity. Other surface modifications may include materials so as to improve biocompatibility [62]. Many materials have been used in several experiments although few act as dispersing agents in aqueous solutions in an efficient and lasting way. The most commonly studied polymers for MNP coating for biomedical applications are dextrin [15, 57] and polyethylene glycol (PEG) [7, 16, 49, 56, 59, 68].

In the present work the Massart method (chemical co-precipitation) was utilized for the synthesis of the MNPs. Variations of the reaction time and stirring conditions were tested in order to determine possible improvements on the established method. A Gum Arabic co-precipitation synthesis was also tested in order to assess the reduction in

nanoparticle agglomeration during synthesis. Nanoparticle characterization was performed using Dynamic Light Scattering (DLS), Transmission Electron Microscopy (TEM), Fourier Transformed Infra Red spectroscopy (FTIR) and Brunauer, Emmett and Teller (BET) analysis.

2.2. Materials and Methods

2.2.1. Materials

Iron (III) chloride hexahydrate ($FeCl_3.6H_2O$), Iron (II) chloride tetrahydrate ($FeCl_2.4H_2O$) and Ammonium hydroxide solution puriss. p.a., 25% NH_3 in H_2O (NH_4OH) were purchased from Fluka. Gum Arabic and KBr were purchased from Sigma-Aldrich.

2.2.2. Equipments

Solid reagents were weighed in an Analytical Balance Sartorius BL6100. Magnetic nanoparticle synthesis was performed using an Electronic Overhead Stirrer RZR 2051 Control from Heidolph. Sonication of MNPs solutions was performed in a Bandelin Sonorex super RK25577 sonicator. Size distribution and Zeta Potential measurements of nanoparticle samples were performed in a Dynamic light scattering Zetasizer Nano ZS from Malvern. FTIR spectra were performed in a Satellite FTIR Mattson Spectrometer**.** Transmission electron microscopy of the nanoparticle samples was performed in an Analytical TEM Hitachi 8100 with Rontec standard EDS detector and digital image acquisition. BET analysis was performed in a Micromeritics ASAP2010 analyzer.

2.2.3. Methods

2.2.3.1. Synthesis of Magnetic Nanoparticles at different reaction times

Magnetic nanoparticles were synthesized using a 1:2 molar ratio of Fe^{2+} to Fe^{3+} [59]. In a closed reactor with stirring at about 1230 rpm, a solution of 570 ml de-ionized water and 30 ml of NH_4OH (0.7 M) was purged with N_2 gas for 30 minutes. After this period, a freshly prepared iron solution (3.29g of $FeCl_3$ and 2g of $FeCl_2$, 30 ml) in de-ionized

water was added drop wise to the ammonium hydroxide solution. The reaction proceeded up to 4,5 hours under a continuous flow of N_2 (Figure 2-1 (a)). A sample was taken every 30 minutes and the pH was monitored and maintained at 10 by the addition of NH_4OH solution. Afterwards, the particles were left to deposit by means of a magnet at room temperature (Figure 2-1 (b)-(c)). The supernatant was discarded and the particles washed several times with de-ionized water to remove the ammonia left in solution. The nanoparticle solution in de-ionized water was kept at 4ºC until further use. Dynamic light scattering (DLS) and Zeta potential measurements were used for MNP sample characterization.

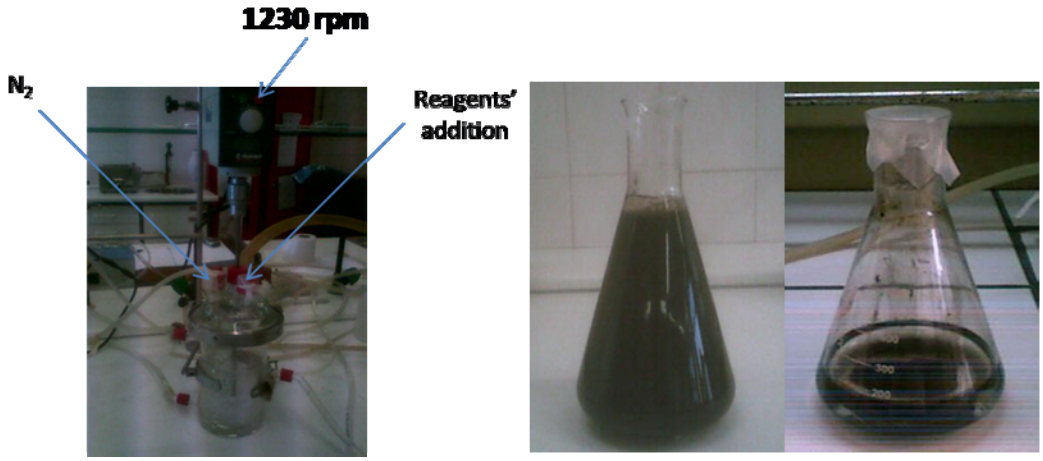

Figure 2-1 (a) Massart's Synthesis equipment; (b) Nanoparticle (MNP) solution as taken from the reactor; (c) Washing of MNP solution with deposition of magnetic nanoparticles by means of a magnet.

2.2.3.2. Synthesis of Magnetic Nanoparticles with different stirring conditions

Magnetic nanoparticles (MNP) were synthesized as described in 2.2.3.1. with the exception that the stirring speed was varied during synthesis (600, 1230 and 1600 rpm). Also, the reaction proceeded up to 4,5 hours under a continuous flow of N_2 and samples were taken at 2 and 4,5 hours.

2.2.3.3. Synthesis of Magnetic Nanoparticles by co-precipitation with GA

Magnetic nanoparticles (MNP) were synthesized as described in 2.2.3.1. with the exception that a GA solution was added during the synthesis. An aqueous solution of Gum Arabic (30 ml, 40 mg/ml) was added to the reaction vessel after addition of the

iron oxide solution. The reaction proceeded up to 4,5 hours and samples were taken at 2 and 4.5 hours.

2.2.3.4. Characterization of synthesized Magnetic Nanoparticles

Nanoparticles synthesized by the methods described in sections 2.2.3.1 to 2.2.3.3 were characterized using DLS, TEM, FTIR and BET analysis.

DLS was utilized for the determination of hydrodynamic size and zeta potential values of MNPs. These indicate the size distribution of MNPs and the electrokinetic potential in colloidal systems (an indication of colloidal stability), respectively. Nanoparticle samples with a final concentration of 1 mg/ml in distilled water were filtered through a 30 μm pore filter. Before each measurement, samples were sonicated and the sample chamber was washed with deionized water to remove any residues.

The TEM analysis was utilized for the characterization of particle morphology and estimation of the size of the magnetic core. The nanoparticle samples were dried under vacuum for 5 hours. The dried nanoparticle samples were observed by Eng. Isabel Nogueira (IST – UTL). All samples were prepared by evaporating dilute suspensions on a carbon-coated film.

FTIR spectra were generated for untreated magnetite nanoparticles as well as those nanoparticles precipitated with Gum Arabic to help identify the differences between functional groups of the various samples. Nanoparticles were dried under vacuum for 5 hours. Nanoparticle samples were prepared as a crushed powder weighing approximately 1 mg and mixed together with 100 mg of crushed KBr. Spectra were taken between 500 and 4000 cm^{-1}.

The specific surface area was determined by Prof. Isabel Fonseca (FCT-UNL) by BET analysis. The nanoparticles were vacuum dried for 5 hours and the surface area was determined by adsorption of N_2 gas on the magnetic nanoparticles at 77K.

2.3. Results and Discussion

The main goal of the studies on the MNP synthesis was to prepare dispersed particles at the nanometer scale. In order to choose suitable protocols for nanoparticle synthesis two parameters were considered: particle size and Zeta potential values. Particles with Zeta potentials more negative than -30 mV or more positive than +30 mV were considered stable [93]. Nanoparticles synthesized at different times and by varying stirring conditions were analysed by DLS and TEM. In Figure 2-2 plots of particle size and Zeta potential as a function of time of synthesis are respectively presented.

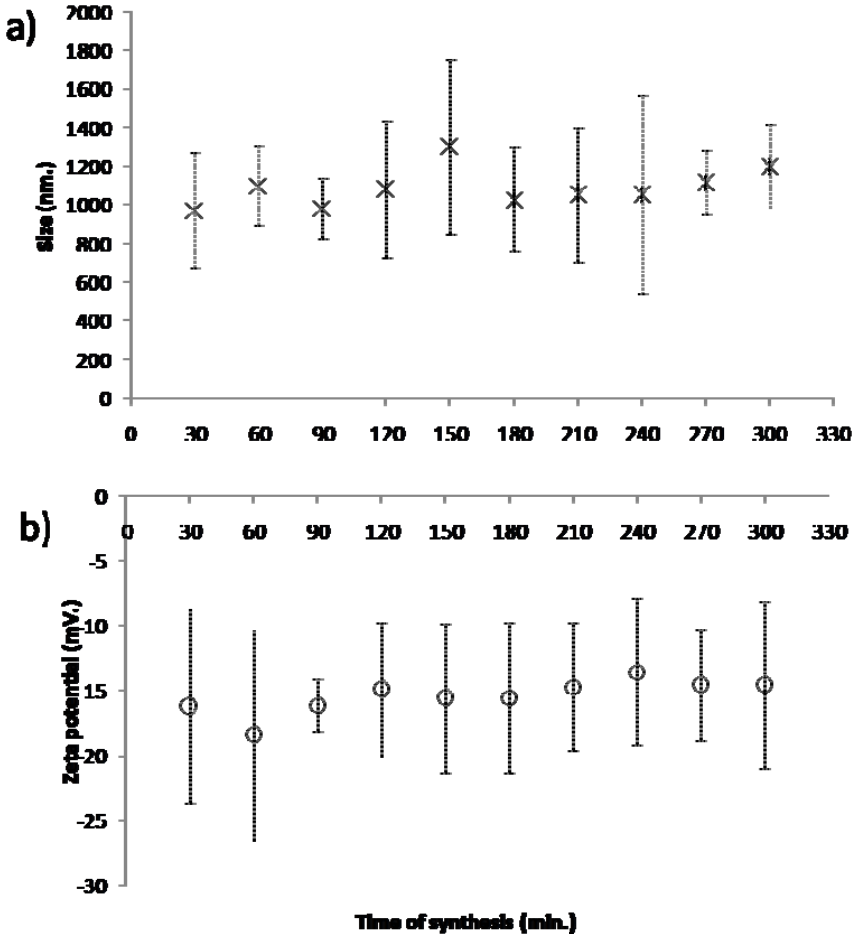

Figure 2-2 Massart synthesis results. (a) Particle size as a function of time of synthesis (n=12); (b) Zeta Potential as a function of time of synthesis (n=12).

Varying the reaction time from 30 to 300 minutes at a constant stirring of 1230 rpm it can be seen that nanoparticle sizes and Zeta potentials vary from 973 ± 298 to 1302 ± 453 nm and -13,6 ± 5,7 to -18,4 ± 8,1 mV, respectively. The errors associated with the

size distribution and Zeta potentials are high comparing to the values they are referring to, but there is no evident variation of these parameters with time. The size and zeta potential values stabilize after 120 minutes of reaction time.

Further studies were addressed, by varying stirring conditions for a 2 and 4,5 hours reaction. In our laboratory, it was previously observed that particles synthesized at periods shorter than 2 hours presented low magnetic response [94]. Accordingly, a 2 hour reaction time was chosen. A 4,5 hours reaction time was used for comparison. The commonly used stirring speed is at 1230 rpm and therefore was selected as a starting point for variation. The variation of particle size and zeta potential as a function of stirring conditions and time are presented in Table 2-1.

Table 2-1 Massart's synthesis results: Particle size and Zeta potentials as a function of stirring speed and time of synthesis

Stirring	**600 rpm (n=1)**		**1230 rpm (n=3)**		**1600 rpm (n=1)**	
Time (min)	Size (nm)	Zeta (mV)	Size (nm)	Zeta (mV)	Size (nm)	Zeta (mV)
120	933±53	-15,8±0,7	923±128	-14,2±4,2	1014±202	-15,7±1,8
270	1091±156	-18,8±0,9	982±354	-14,8±1,5	1183±75	-14,5±2,6

The results presented in Table 2-1 show that the nanoparticle sizes for all the stirring conditions tested (600, 1230 and 1600 rpm) are similar, although the nanoparticle size obtained in the 2 hour synthesis is lower for the nanoparticles synthesized at 1230 rpm. The zeta potential values for the 2 and 4,5 hour reaction is less negative for the 1230 rpm samples, and more negative for the other stirring speeds, specially the 600 rpm, for the 2 and 4,5 hour reaction. The zeta potentials varied between -14,2 ± 4,2 and -18,8 ± 0,9 mV, within the +30 to -30 mV range that is related to nanoparticle instability in solution. The approximation to more negative zeta potentials (-30 mV) shows a tendency to an increase in particle stability [93].

Comparing the two sets of results and considering previous work, the conditions for the nanoparticle synthesis in our laboratory setting were selected as 2 hours of reaction time with 1230 rpm of stirring speed. With these conditions it is possible to prepare small particles with negative zeta potential values. Although the zeta potential results are not

as favorable as the size results for the chosen conditions, a small nanoparticle size was considered more important than stability as a parameter for the optimization of MNP synthesis. This is because small particles are usable in many applications and the stability of MNPs may be improved later with an appropriate surface modification of the synthesized nanoparticles [19].

The nanoparticle synthesis was performed for 2h reaction time, with 1230 rpm stirring speed and the synthesized nanoparticles were further characterized by DLS, TEM, FTIR and BET analysis. The DLS experiments were repeated on the same MNPs one month after synthesis. The MNPs presented an average size of 1477 ± 136 nm, showing minor peaks at 200 nm and 5000-6000 nm, which reflects the formation of agglomerates after particle synthesis leading to a greater sample heterogeneity. The correspondent zeta potential values were 19,6 ± 1,2 mV, which apparently reflects an improvement in colloidal stability.

In order to characterize the morphology and size of the particles, samples were analyzed at random by TEM, and microscopy photographs (micrographs) were taken at different amplifications (Figure 2-3). As expected, the nanoparticles presented a spherical morphology [57, 93-95]. The average primary particle size was 11 ± 3 nm in good accordance with the 8.0 ±1 nm values obtained by Predoi et al. (2007) [57], 8-10 nm obtained by Iida et al. (2007) [95] and 5–10 nm obtained by Ma et al. (2007) [94].
Agglomerates of MNPs can be observed, which are most likely formed during MNP synthesis. Figure 2-3 (a)) shows a larger fragment of agglomerated MNPs (2652 nm), a higher value than the one obtained in DLS measurements. The discrepancy in diameters of MNP agglomerates may be due to the nature of the analytical method. In DLS, a filtered aqueous solution of nanoparticles is analyzed, larger aglomerates tend to deposit on the bottom of the DLS cell and the smaller agglomerates are dispersed in solution and thus measured. In TEM, it is possible to analyze every fragment however large it may be, because the nanoparticle solution is evaporated in the carbon-coated film.

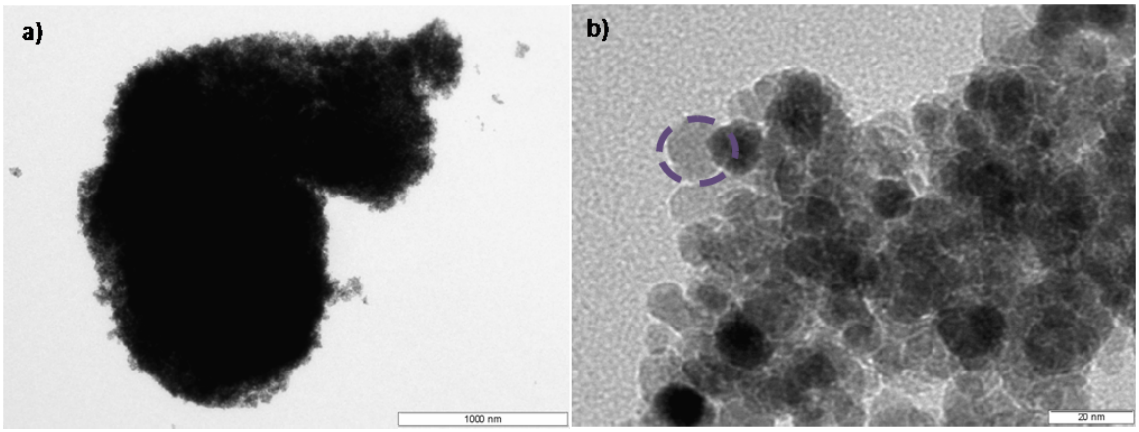

Figure 2-3 TEM micrographs of magnetic nanoparticles taken at different magnifications (a) cluster of particles; (b) dotted circle indicates a single particle witthin the cluster.

The BET analysis of the magnetic nanoparticles synthesized by the Massart's method resulted in a specific area of 908 m^2/g, a micropore volume of 0,65 cm^3/g and a total pore volume of 0.83 cm^3/g.

The FTIR spectrum of the iron oxide nanoparticles showed characteristic OH stretching (ν OH) and HOH bending (δ OH) vibrational bands at 3443 cm^{-1} due to the adsorbed water in the sample. A peak at 1614 cm^{-1} is identified. A ν(Fe-O) peak is observed for the bare magnetite sample at 571 cm^{-1} .

In order to assess the effect of GA addition in particle size, morphology and dispersion during MNP synthesis, GA-co-precipitated magnetic nanoparticles were synthesized by the Massart method, at 1230 rpm for a 2 hour reaction period. These particles were analyzed using DLS, TEM and FTIR soon after synthesis (MNP_GA) and several days after (23 days) synthesis (MNP_GAagg), allowing for MNP agglomeration to occur. Size distribution and Zeta potential results for the GA-co-precipitated MNPs are presented in Table 2-2.

Table 2-2 Size distribution and zeta potential results for bare magnetite and the Gum Arabic-co-precipitated magnetic nanoparticle synthesis (n=3).

Sample	Size (nm)	Zeta potential (mV)
MNP	923±128	-14,2±4,2
MNP_{agg}	1477±136	-19,6±1,2
MNP_GA	341±69	-22,1±2,8
MNP_GA_{agg}	1108±263	-13,4±2,1

The GA-co-precipitated MNPs are clearly smaller than bare magnetite. On the other hand, as previously observed, the MNPs analyzed approximately one month after synthesis reflected agglomeration. There are minor peaks at 100-200 nm and 5000-6000 nm, showing some degree of heterogeneity in the GA-co-precipitated MNP samples. These results contradict the ones obtained by Williams et al. (2006) [62] and Wilson et al. (2008) [59], as in these works larger agglomerates were obtained for GA-co-precipitated nanoparticles than for bare magnetite nanoparticles. These agglomerates presented an average size of 1000 nm which is within the range of the MNP_GA_{agg}. The agglomeration of GA-co-precipitated MNPs after synthesis may be due to complex bridging interactions, formed when part of the large GA molecule is adsorbed onto the surface of two or more particles [62].

Comparing the zeta potential values for the GA-co-precipitated MNPs and bare magnetite before agglomeration, it is clear the stabilizing effect of GA [62]. However, after agglomeration occurs two sets of results can be observed. For the bare magnetite particles, the agglomeration leads to a more negative zeta value. For the GA-co-precipitated MNPs, the agglomeration leads to less negative zeta values and therefore a loss of colloidal stability.

Particle size and morphology were analyzed by TEM. The resulting micrographs taken with different amplifications are shown in Figure 2-4, where it is possible to observe the spherical morphology of the GA-co-precipitated nanoparticles. The average primary particle size was 14 ± 4 nm, within the same range described by Banerjee et al. (2007) [30] for GA modified MNPs (13 – 67 nm range with an average diameter of 34 nm (± 5%)). This also reflects an increase in diameter from the bare magnetite particle size (11

± 3 nm). In the micrographs (Figure 2-4 (a)-(b)) smaller agglomerates of MNPs (950 nm) are observed in comparison with those observed in bare magnetite particles.

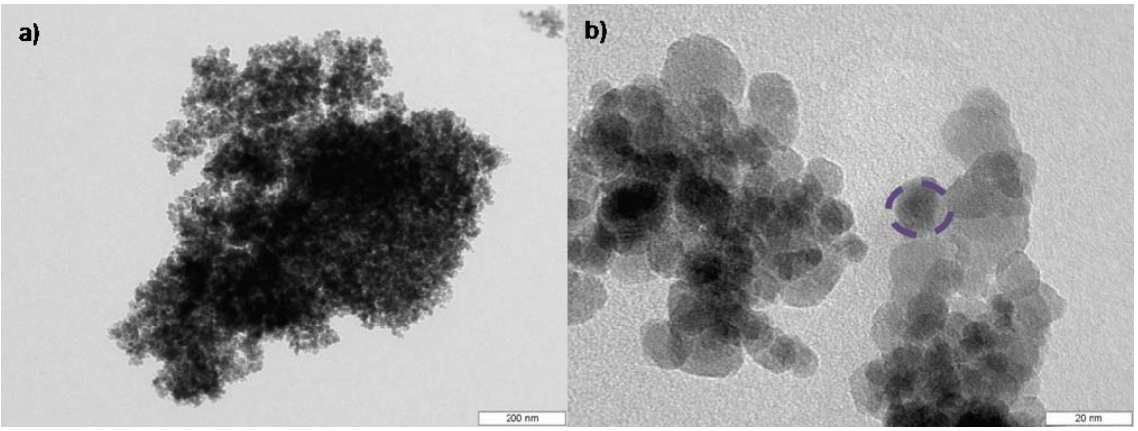

Figure 2-4 TEM micrographs of GA-co-precipitated magnetic nanoparticles taken at different magnifications (a) cluster of particles; (b) dotted circle indicates a single particle witthin the cluster.

A FTIR spectrum was generated for Gum Arabic and for GA-co-precipitated nanoparticles so as to identify the functional groups present in the samples. The FTIR results for the bare magnetite nanoparticles, Gum Arabic and GA-co-precipitated magnetic nanoparticles are comprised in Table 2-3.

Table 2-3 Comparison of FTIR results obtained for bare magnetite nanoparticles, Gum Arabic and GA-co-precipitated nanoparticles.

MNP opt (cm^{-1})	GA-co-precipitated MNP (cm^{-1})	GA (cm^{-1})
3450	3443	3450
-	-	2926
2371 – 2272	2329	2397 – 2349
1614	1614	1638 – 1600
-	-	1424
-	-	1032 – 1076
-	1000	977
571	571	552

The analysis of the FTIR spectra was not facilitated by the superposition of many peaks characteristic of GA and MNPs. From FTIR results, it can be seen that, the spectrum of the iron oxide nanoparticles (untreated and treated) and Gum Arabic contain characteristic OH stretching (ν OH) and HOH bending (δ OH) vibrational bands at 3443 - 3450 cm^{-1} due to the adsorbed water in the sample. The 2926 cm^{-1} peak in GA is characteristic of stretching vibrations of the C-H bond (ν C-H of $–CH_2$). In GA the absorption band at 2397 – 2349 cm^{-1} is usually due to CO_2 vibration. A carboxylate group associated with the Gum Arabic molecule shows a strong peak at 1600 - 1638 cm^{-1} (C=O stretch and N-H bending) in GA sample [43] and a peak at 1614 cm^{-1} is identified in optimized MNP and GA-co-precipitated MNP. Bands in the regions of 1424, 1000 and 977 cm^{-1} in GA and GA-co-precipitated MNPs are due to the C-O bond stretch indicating GA presence in GA-co-precipitated MNPs. A ν(Fe-O) peak is observed for the bare magnetite sample at 571 cm^{-1}. A superposition of a GA peak at 552 cm^{-1} with a characteristic ν(Fe-O) peak (566) [30, 57, 68, 96] at 571 cm^{-1} is observed for the GA-co-precipitated MNP sample. Adsorption bands for amine groups in GA, bands due to N-H stretch for primary amine (3400 - 3500 cm^{-1}) and secondary amine (3310 – 3350 cm^{-1}), have not been clearly identified in these samples. An explanation possible is that Gum Arabic is made up of a high molecular weight glycoprotein and a higher amount of a lower molecular weight polysaccharide and the adsorption bands due to the N-H stretch may be covered by the broad adsorption band at 3000 – 3600 cm^{-1} due to the O-H stretch of the polysaccharide [97] . These results confirm the success of the adsorption of GA onto bare MNPs.

2.4. Conclusions

For the synthesis of bare nanoparticles (MNP), a time of reaction of two hours at a constant stirring of 1230 rpm with a continuous flow of N_2 was chosen. These conditions were also applied successfully for the synthesis of magnetic nanoparticles co-precipitated with Gum Arabic (MNP_GA). The mean diameters obtained by TEM for MNP (11 ± 3 nm) and MNP_GA (14 ± 4 nm) are in the nanometric range, although MNPs aggregates are formed during (MNP_{agg}) and after synthesis (MNP_GA_{agg}), presenting higher average values (2652 and 950 nm respectively). The hydrodynamic sizes obtained by DLS, indicate an approximately 3-fold decrease for the MNP_GA.

Aggregates formed during time after synthesis for bare magnetite (MNP_{agg})(1477 ± 136 nm) displayed higher sizes compared to GA-co-precipitated nanoparticle aggregates (MNP_GA_{agg})(1108 ± 263 nm). Zeta potential measurements provided further confirmation of Gum Arabic contribution to MNP stability in aqueous solution. Zeta potential values obtained for MNP and MNP_GA showed an increase in the MNPs dispersivity provided by GA during MNPs synthesis. GA-co-precipitated MNP agglomeration over time led to an increase in zeta potential values, showing a reduction in nanoparticle stability in solution due to particle agglomeration. Gum Arabic presence in MNP_GA was identified by FTIR spectra, as a characteristic GA peak (977 cm^{-1}) was observed in GA-co-precipitated nanoparticle samples (MNP_GA) at 1000 cm^{-1}.

In order to enhance iron oxide nanoparticle stability, an appropriate coating is required during nanoparticle synthesis or post-synthesis. From the results obtained in this study it is possible to say that GA displays potential as a coating material for reducing the agglomerate formation during MNP synthesis and improving particle stability in solution. After synthesis, treatment of bare magnetite (MNP) with Gum Arabic is also possible and will be addressed in Chapter 3.

Chapter 3 – Surface Modification of Magnetic Nanoparticles with Gum Arabic

3.1. Introduction

Magnetic nanoparticles (MNPs) have a tendency to aggregate during and after synthesis as a way to reduce surface energy. In order to prevent nanoparticle aggregation and to improve biocompatibility, the surface of the magnetic nanoparticles can be modified with polymers such as dextrin [15, 57], polyethyleneglycol (PEG) [7, 16, 49, 56, 59, 68], oleylamine [59], chitosan [52-55], oleic acid [55, 67], dextran [48, 56] and albumin [15, 50]. Recently, a polymer known as Gum Arabic (GA) has been shown to sustain colloidal stability for carbon nanotubes in aqueous solutions [61], to act as a steric stabilizer in the preparation of colloidal copper particles [53], and in the stabilization of MNPs [28, 59, 62]. GA is found in nature as a mixture of calcium, magnesium and potassium salts of a polysaccharide acid (Arabic acid). It is predominantly a carbohydrate with about 2% of protein rich in hydroxyprolyl, prolyl and seryl residues, being responsible for its emulsifying activity [73, 98]. GA has a waddle-blossom structure with a number of polysaccharide units (blocs) linked to a common polypeptidic chain.

In the present work GA was used for the surface modification of MNPs in order to assess its effect on minimizing agglomeration events after MNPs synthesis. Surface modification with GA was achieved in two ways: adsorption and covalent coupling. The former was performed on bare magnetite MNPs (MNP_GA_{ADS}) and on MNPs co-precipitated with GA (MNP_GA_GA_{ADS}), the latter was obtained either via reaction of GA amine groups with aldehyde functionalized nanoparticles (MNP_GA_{APTS}), or via reaction of GA carboxylic groups with amine functionalized nanoparticles (MNP_GA_{EDC}). Nanoparticle characterization was performed using Dynamic Light Scattering (DLS), Transmission Electron Microscopy (TEM), Fourier Transformed Infra Red spectroscopy (FTIR) and Brunauer, Emmett and Teller (BET) analysis.

3.2. Materials and methods

3.2.1. Materials

APTS (3-Aminopropyl) triethoxysilane, 99% (lot 12915KD-106), Gum Arabic, N', N'' – dimethylformamide (DMF) ≥99,8% A.C.S Reagent (319937) and KBr were purchased from Sigma-Aldrich.

Acetone p. a. (44477), Dimethylsulphoxide (DMSO) puriss p. a. ≥99,5% (GC) (41644), EDC (N-(3-dimethylaminopropyl)-N'-ethylcarbodiimide) (39391), Hydrochloric Acid (84426), Ninhydrin puriss p.a. ≥99% (33437), Phenol purum ≥99,0% (GC) (77612) and Potassium cyanide puriss p. a. ≥98,0% (AT) (60179) were purchased from Fluka.

Bicinchoninic Acid Kit for Protein Determination (BCA1) for 200-1000 μg/ml protein (096K9802), 6-APA (ε-Amino-n-caproic acid) (A-2504), Glutaraldehyde 50 wt. % in H_2O (lot S36104-217) and Sodium Hydroxide, reagent grade, 97%, beads (367176) were supplied by Sigma.

Sodium Chloride puriss p.a. (31434) was purchased from Riedel de Haën.

Sodium dihydrogen phosphate monohydrate (NaH_2PO_4 * H_2O) (A896946607) and Sodium tetraborate ($Na_2B_4O_7$) (6306 – A655106) were supplied by Merck.

3.2.2. Equipments

Solid reagents were weighed in an Analytical Balance Sartorius BL6100. Nanoparticle solution sonication was performed in a Bandelin Sonorex super RK25577 sonicator. The amination reaction, Kaiser and TNBS tests were performed in a water-bath from Memmert. Gum Arabic stock solution and Nanoparticle solution centrifugations were performed in a Beckman Avanti Centrifuge J-25 – Beckman Rotor JA-25-50 and in an Eppendorf Centrifuge 1-15K from Sigma Sartorius, respectively. Throughout the laboratory work solutions were homogenized with Magnetic stirrer KMO2 electronic Janke Kunkel IKA from Labortechnik and with a Vortex TM1 from Techmatic. During functionalization reactions, samples of nanoparticle solution were shaken in a Swinging Shaker Rotabit from P Selecta.

Nanoparticle samples were dried overnight in an Oven/ stoof U 15 (maximum 220ºC) from Memmert.

Spectrometric readings were performed in a Helios Alpha UV-Vis spectrophotometer from Spectronic Unicam (Thermo Unicam) in cuvettes UV transparent from 220 nm (D-51588) from Sarstedt. Readings of microplates were performed in a Microplate reader Infinite M200 from Tecan with i-control interface software. Size distribution and Zeta Potential measurements of the nanoparticle samples were performed in a Dynamic light scattering Zetasizer Nano ZS from Malvern. FTIR spectra were performed in a Satellite FTIR Mattson FTIR Spectrometer**.** Transmission electron microscopy (TEM) of the nanoparticle samples was performed in an Analytical TEM Hitachi 8100 with Rontec standard EDS detector and digital image acquisition. BET analysis was performed in a Micromeritics ASAP2010.

3.2.3. Methods

3.2.3.1. Characterization of Gum Arabic in Aqueous Solution

In order to determine the concentration of free carboxylic acid groups in Gum Arabic solutions, titrations with NaOH 0,05 M were performed. The pH value for a 40 mg/ml GA solution at room temperature is 4,52. A volume of 0,475 ml of NaOH 0,05 M was added to 10 ml of 40 mg/ml GA solution, yielding $5{,}9\times10^{-8}$ moles COOH/mg GA.

The concentration of free amine groups in GA was determined by the Kaiser test. The Kaiser test is a qualitative test for the presence or absence of free primary amino groups. The test is based on the reaction of ninhydrin with primary and secondary amines, which gives a characteristic dark blue colour. In the absence of free amine groups a yellow colour is obtained. The test requires minimal amounts of analyte and is completed within a few minutes [99, 100]. The following reagents (50µl each) were added to 1ml of an aqueous solution of GA 40 mg/ml: Phenol 80% in ethanol solution (w/v), KCN in H_2O/pyridine (2% v/v) and Ninhydrin 5% in ethanol (w/v). The solution was incubated at 120ºC in a water-bath for 5 minutes. The blank was a 1ml solution of water. The absorbance of the supernatant was measured at 570 nm. Different solutions of 6-amino caproic acid (0; 0,6; 1,25; 2,5; 5, 10, 20 µmol/ml) were used to build a calibration curve (Abs=0,056*C-0,018 (R^2=0,979); n=3). The typical values for the concentration of free amine groups in GA were 6×10^{-7} mol [NH_2]/mg GA.

The concentration of GA in aqueous solutions was determined by the microplate bicinchoninic acid test (BCA test) [101]. The BCA reagent for was freshly prepared by mixing reagent A and B in a 50:1 proportion [28]. 50 µl of the samples to be tested were individually added to wells of a 96-well microplate. Then, 200 µl of the BCA reagent were added to each well. The microplate was incubated in the dark at 37ºC for 20 minutes. Absorbance was read at 562 nm and for each assay a calibration curve with GA Standards (0-70 mg/ml) was performed. The calibration curve obtained was Abs=0,014*C+0,021, R^2=0,998 (n=10).

3.2.3.2. Adsorption of Gum Arabic onto Magnetic Nanoparticles

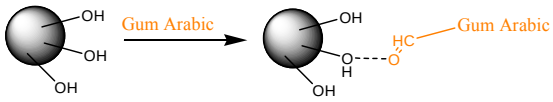

Figure 3-1 Gum Arabic adsorption onto magnetic nanoparticle surface.

Solutions of MNPs (MNP and MNP_GA) (14x1ml of 12 mg/ml nanoparticle suspension) were placed in 14 Eppendorf tubes and washed 6 times with de-ionized water. The volume was completed with 1 ml of standard solutions of GA (0-70mg/ml). The MNP solutions were shaken, sonicated at 10 Watts for 10 minutes and incubated for 1 hour at room temperature under orbital shaking. The solutions were then washed 3 times with de-ionized water, supernatants were removed and stored. The samples were centrifuged in each washing step at 9167g for 15 to 20 minutes. The supernatants were analyzed using the microplate BCA method to determine GA adsorption onto MNPs. DLS, TEM and FTIR were used for MNP characterization (see Chapter 2).

3.2.3.3. Covalent Coupling of GA onto Aldehyde functionalized Nanoparticles (MNP_GA_{APTS})

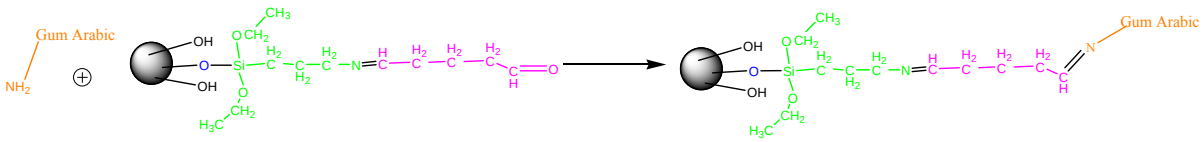

Figure 3-2 Covalent coupling between Gum Arabic and functionalized MNPs

MNPs were aminated with APTS reagent. An appropriate volume of nanoparticle solution (14 ml of 12 mg/ml nanoparticle suspension) was washed 6 times with distilled water. The supernatants were discarded and the volume was completed with de-ionized water (14 ml). APTS (2968 µl, 0.4% v/v) was added to the nanoparticle solution. The solution was shaken, sonicated at 10 watts for 10 minutes and incubated for 1 hour at 70ºC in a water-bath [41]. After incubation, the nanoparticle sample was washed 6 times with de-ionized water and the volume was completed with de-ionized water (14 ml). The amount of amine groups at the surface of the MNPs was determined by the Kaiser test using 1ml solutions of MNPs. Typical values were 39,2 ± 11,5 µmol NH_2/mg of nanoparticles.

A volume of 0.775 ml of glutaraldehyde (5% v/v) was added to 14 ml of 12 mg/ml the aminated MNP solution. Glutaraldehyde is added in a 1:1 molar ratio relatively to the aminated MNP concentration determined by the Kaiser test. The solution was shaken, sonicated for 10 minutes and incubated for 1 hour at room temperature with orbital shaking. After incubation, the solution was washed 6 times with de-ionized water, the volume was completed with de-ionized water (14 ml). This solution containing aldehyde-functionalized MNPs was divided in 14 aliquots. The particles were left to deposit and the supernatant removed.

A 1 ml solution of GA (0-70 mg/ml) was added to each aliquot of aldehyde-functionalized MNPs. Samples were shaken, sonicated at 10 watts for 10 minutes and incubated for 1 hour, at room temperature, with orbital agitation. After incubation, samples were washed 3 times with de-ionized water, supernatants were removed and stored. The samples were centrifuged in each wash at 9167 g for 15 to 20 minutes. The supernatants were analyzed using the microplate BCA method to determine GA deposited at the MNPs surface. DLS, TEM and FTIR were used for MNP characterization (see Chapter 2).

3.2.3.4. Covalent Coupling of EDC activated Gum Arabic onto amine functionalized Nanoparticles (MNP_GA$_{EDC}$)

A solution of EDC (73µl, 3 equivalents excess of the amount of aminated MNPs) in de-ionized water (1ml) was prepared, and a volume of 91 µl was added to each standard solution of Gum Arabic (1 ml, 0 - 70 mg/ml) and incubated for 15 minutes (Solution A). 14 ml of MNPs functionalized with amines [41] were divided in 14 aliquots (Solution B). The particles were left to deposit and the supernatant removed. A volume of 1 ml of activated-GA (0-70 mg/ml) (Solution A) was added to each aliquot. Samples were shaken, sonicated at 10 watts for 10 minutes and incubated for 2 hours, at room temperature, with orbital agitation. After incubation, samples were washed 3 times with de-ionized water, supernatants were removed and stored. The samples were centrifuged in each wash at 9167 g for 15 to 20 minutes. The supernatants were analyzed using the microplate BCA method to determine GA deposited at the MNPs surface. DLS, TEM and FTIR were used for MNP characterization (see Chapter 2).

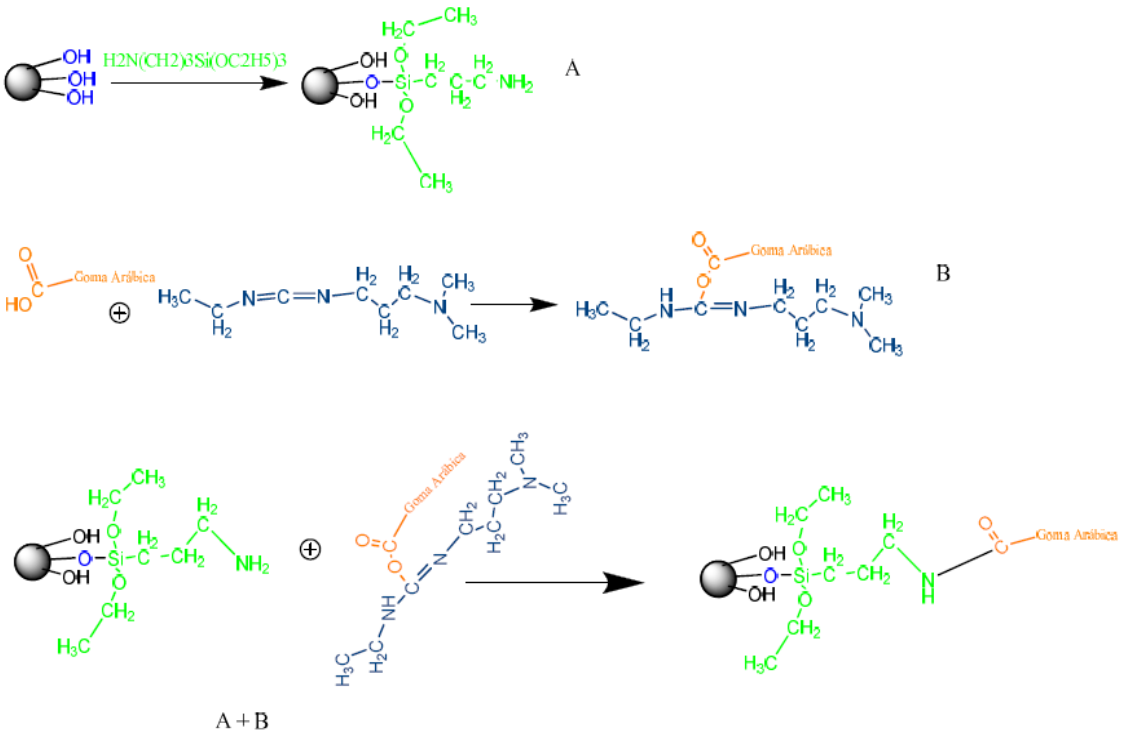

Figure 3-3 Covalent coupling between aminated MNPs and EDC functionalized Gum Arabic

3.2.3.5. GA Displacement Studies

Samples of MNP_GA_{ADS}, MNP_GA_GA_{ADS}, MNP_GA_{APTS} and MNP_GA_{EDC} were tested. A phosphate buffer stock solution was prepared (1 M $NaH_2PO_4.H_2O$ and 150 mM NaCl) in de-ionized water. Phosphate buffer standard solutions 100, 10, 1 and 0,1mM were prepared with pH 7,5. Supernatants of MNP sample (1ml) were discarded and 1 ml of phosphate buffer solutions (1000, 100, 10, 1 and 0.1 mM) were added. Samples were shaken, sonicated at 10 watts for 10 minutes and incubated at room temperature for 2 hours in a orbital shaker. After incubation, samples were washed 2 times with de-ionized water and the supernatants were kept. In each washing the samples were centrifuged at 9167 g for 15 to 20 minutes. The supernatants were analyzed using the microplate BCA method to determine GA concentration left in solution (3.2.3.2.).

3.3. Results and Discussion

The quantity of free amine groups present in a 40mg/ml aqueous solution of GA (6×10^{-7} mol [NH_2]/mg GA) was ten-fold the quantity of carboxylate groups ($5{,}9\times10^{-8}$ moles COOH/mg GA). The different amount of amines and carboxylate groups in GA may account for the different values obtained for the covalent coupling either via reaction of GA amine groups with aldehyde functionalized nanoparticles (MNP_GA_{APTS}), or via reaction of GA carboxylic groups with amine functionalized nanoparticles (MNP_GA_{EDC}).

The MNPs were functionalized with GA utilizing different methods. Bare magnetite (MNP) were either used for direct adsorption of GA or for covalent attachment of GA. Particles co-precipitated with GA during synthesis (Chapter 2) were also further functionalized with GA by the adsorption method. In order to compare the maximum amount of GA deposited at the surface of MNPs, adsorption isotherms were constructed for each coupling method Figure 3-4.

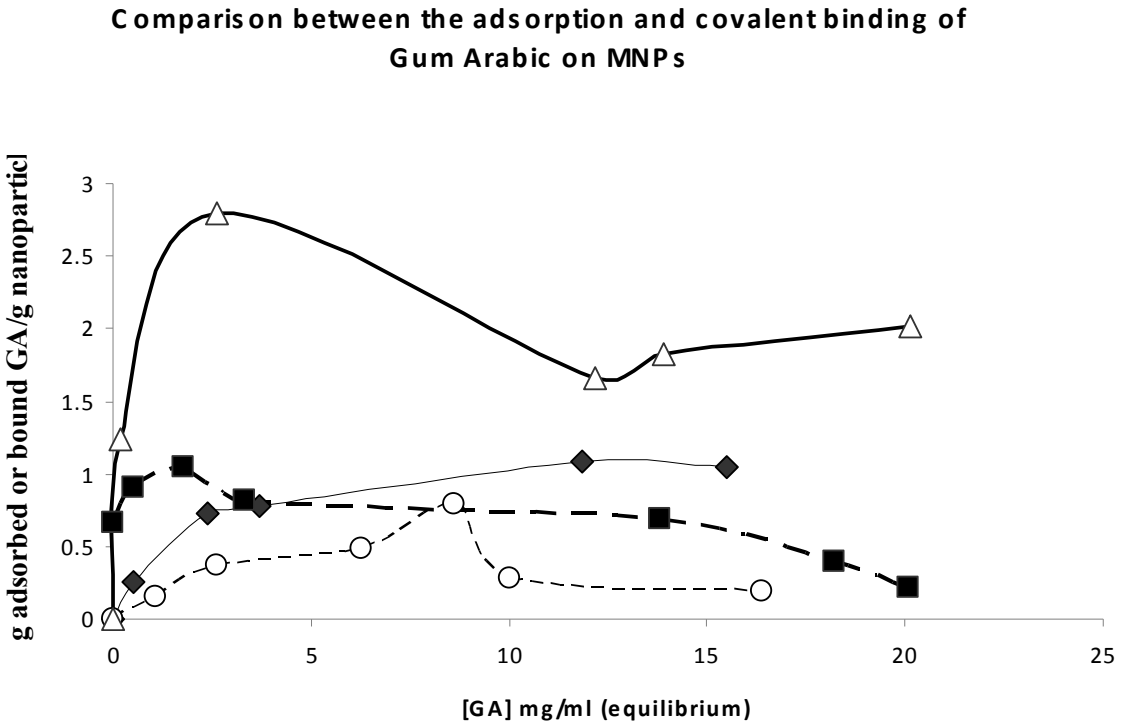

Figure 3-4 Adsorption isotherms of GA at the surface of MNPs using different methods. Key: ♦ - GA adsorbed on MNPs; ○ - Covalent binding of GA on glutaraldehyde functionalized MNPs; Δ - Covalent binding of GA on aminated MNPs; ■ - GA adsorbed on GA-co-precipitated MNPs.

The adsorption isotherms followed a Langmuir pattern. The amount of GA adsorbed per gram of particles was distinct for each method Table 3-1.

Table 3-1 Adsorption and covalent coupling maxima.

Sample	[GA] (eq.) mg/ml	g GA (ads)/ g MNP
MNP_GA_{ADS} (n=4)	11,85 ± 0,59	1,09 ± 0,42
MNP_GA_GA_{ADS} (n=3)	1,78 ± 0,07	1,05 ± 0,21
MNP_GA_{APTS} (n=4)	8,62 ± 0,00	0,79 ± 0,00
MNP_GA_{EDC} (n=2)	2,62 ± 0,00	2,80 ± 0,00

In Table 3-1 a range of 0,79 to 2,80 g GA/ g MNP may be observed for the adsorption and covalent coupling of GA onto MNPs. These values are higher than those reported in literature, where a maximum of 0,6 g GA was adsorbed per gram of MNPs [28]. The maximum of GA deposited at the surface of MNPs was obtained for GA covalently

coupled on amine functionalized MNP (2,80 ± 0,00 g GA /g MNP). This may be due to cross-linking between adjacent GA molecules after EDC activation of Gum Arabic. The carboxyl groups in GA are activated with EDC and may react with the amine groups of other GA molecules forming bridges between neighbor molecules. The remaining activated COOH groups may then react with the amine groups of the MNPs, forming a covalent bond. The maximum of GA adsorption onto bare magnetite, MNP_GA_{ADS} (1,09 ± 0,42 g GA/ g MNP) indicates that GA has a high affinity to the iron oxide surface. The binding interaction between GA and the magnetite nanoparticles is probably due to the Gum Arabic COOH group interaction with the hydroxyl groups of bare magnetite nanoparticles [93]. For the MNP_GA_GA_{ADS} samples, an adsorption maximum of 1,05 ± 0,21 g GA/g MNP is obtained, a value very close to the maxima obtained for MNP_GA_{ADS}. In MNP_GA_GA_{ADS}, it is possible that the adsorbed Gum Arabic forms multilayers around the nanoparticles, explaining the adsorption maximum obtained [28]. The values for GA deposited at MNPs surface here presented are 2 to 6-fold higher than data previously obtained by our group [102]. The main difference between these assays was that in the present studies all nanoparticle samples were sonicated before all functionalization and coating steps. With the sonication, better dispersed nanoparticle samples were prepared, allowing for a better nanoparticle coating with Gum Arabic.

From Figure 3-4, an order of saturation of GA adsorption or covalent coupling may be determined: the first sample to reach a saturation stage of GA coating is GA covalently coupled onto amine functionalized MNPs (MNP_GA_{EDC}), then GA adsorbed onto GA-co-precipitated nanoparticles (MNP_GA_GA_{ADS}), followed by GA adsorbed on MNPs (MNP_GA_{ADS}) and GA covalently bound onto glutaraldehyde functionalized MNPs (MNP_GA_{APTS}). The same order of saturation was obtained previously by our group.

Particle morphology of all studied MNPs (MNP, MNP_GA_{ADS}, MNP_GA_GA_{ADS}, MNP_GA_{APTS} and MNP_GA_{EDC}) was analyzed with TEM. Micrographs were taken at different amplifications (Figure 3-5 (a)-(h)). All samples presented magnetic particles with a spherical morphology. The average diameter of the particles was 14 ± 1 nm, 14 ± 1 nm, 11 ± 3 nm and 12 ± 3 nm for MNP_GA_{ADS}, MNP_GA_GA_{ADS}, MNP_GA_{APTS} and MNP_GA_{EDC}, respectively (Table 3-2). The diameters determined are within the range of 13-67 nm obtained by Banerjee et al. (2007) [30] for GA co-precipitated

magnetic nanoparticles. Agglomerates of nanoparticles were also observed; the 8000X magnification micrographs show a larger fragment of agglomerated MNPs: 1773 nm for the small and 2818 nm for the large agglomerates of MNP_GA_{ADS}, 2045 nm for MNP_GA_GA_{ADS}, 1727 nm for MNP_GA_{APTS} and 1772 nm for MNP_GA_{EDC}.

Table 3-2 Nanoparticle and MNP agglomerate average diameter determined from TEM micrographs.

Sample	MNP Diameter (nm)	Agglomerate Diameter (nm)
MNP	11 ± 3	2652
MNP_GA	14 ± 4	950
MNP_GA_{ADS}	14 ± 1	1773, 2818
MNP_GA_GA_{ADS}	14 ± 1	2045
MNP_GA_{APTS}	11 ± 3	1727
MNP_GA_{EDC}	12 ± 3	1772

From Table 3-2, it is possible to observe that, although the error associated with the average diameters of the GA covalently bound to functionalized MNP are higher (MNP_GA_{APTS} and MNP_GA_{EDC}), these MNP show a smaller average diameter compared to particles with adsorbed GA (MNP_GA_{ADS} and MNP_GA_GA_{ADS}). When GA is adsorbed, the mean diameters of the MNPs tend to be higher, possibly due to the formation of multilayers of polymer.

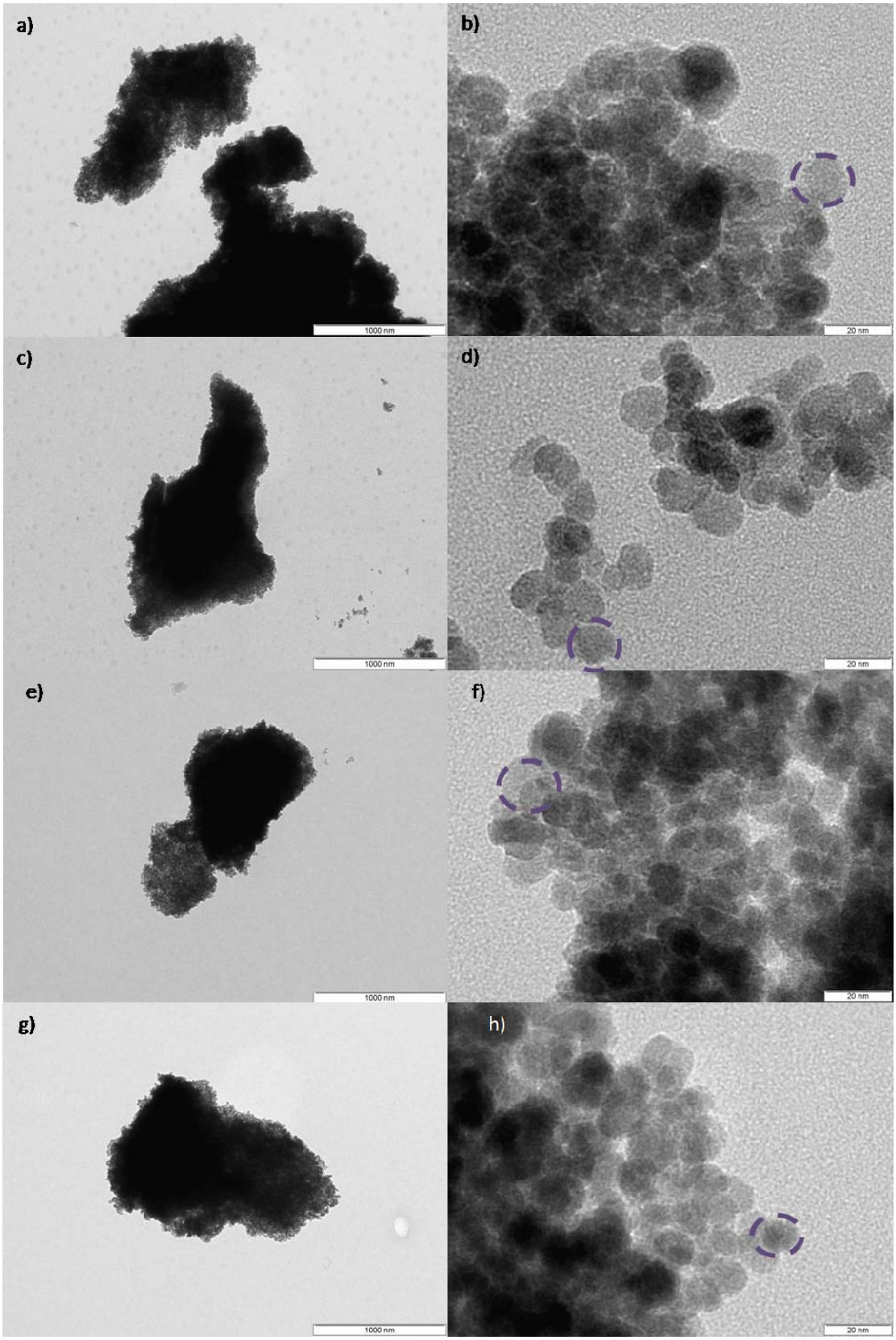

Figure 3-5 TEM micrographs of GA coated magnetic nanoparticles taken at different magnifications: (a), (b) MNP_GA$_{ADS}$; (c), (d) MNP_GA_GA$_{ADS}$; (e), (f) MNP_GA$_{APTS}$; (g), (h) MNP_GA$_{EDC}$. (a), (c), (e), (g) cluster of particles; (b), (d), (f), (h) dotted circle indicates a single particle within the cluster.

Size Distribution and Zeta Potential values for the MNP_GA_{ADS}, MNP_GA_GA_{ADS}, MNP_GA_{APTS} and MNP_GA_{EDC} samples were performed using DLS. The results obtained are comprised in Table 3-3.

Table 3-3 Size distribution and Zeta potential results for the surface modified nanoparticles (n = 3).

Sample	Size (nm)	Zeta (mV)
MNP	1476,67±135,77	-19,63±1,21
MNP_GA	341,33±69,06	-22,07±2,77
MNP_GA_{ADS}	1306,67 ± 41,63	-24,67 ± 1,94
MNP_GA_GA_{ADS}	1128,67 ± 227,74	-26,00 ± 0,78
MNP_GA_{APTS}	1500,00 ± 196,98	-26,63 ± 0,49
MNP_GA_{EDC}	1120,00 ± 60,00	-24,53 ± 0,42

The average hydrodynamic diameter of the MNP_GA_{ADS}, MNP_GA_GA_{ADS}, MNP_GA_{APTS} and MNP_GA_{EDC} are all similar and within the range 1100-1500 nm. These are similar to the value obtained for bare magnetite (MNP). The particles displaying the smallest diameter are those where GA was added during synthesis (MNP_GA).

Zeta potential values for modified MNPs are in the range of -24 to -27 mV, in the proximity of -30 mV, showing an increasing tendency for MNP stabilization comparing to bare magnetite (MNP)(-19,63 ± 1,21 mV) and GA-co-precipitated MNPs before and after aggregation (MNP_GA and MNP_GA_{agg})(-22,07 ± 2,77 mV and -13,37 ± 2,10 mV). The Zeta potential values for GA covalently coupled to aldehyde functionalized MNPs (MNP_GA_{APTS}) show that these nanoparticles are more dispersible and stable in solution than the other samples. These results show that Gum Arabic coating of iron oxide magnetic nanoparticles increase particle stability in solution although aggregation of MNPs still occur over time. In Figure 3-6, Figure 3-7 and Figure 3-8, a summary of the measures obtained using DLS and TEM is presented.

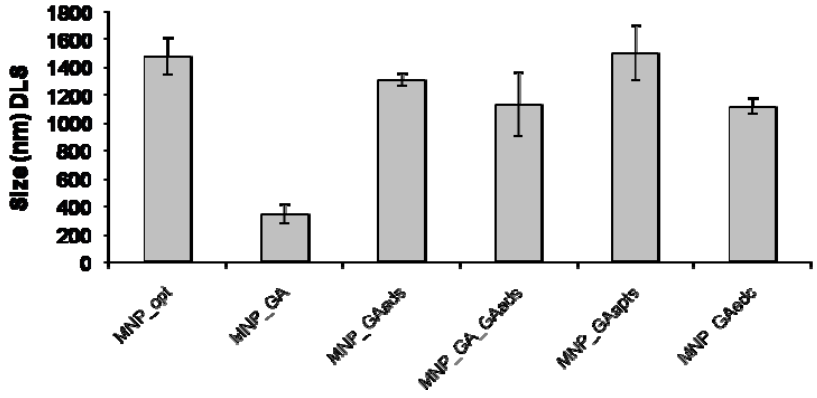

Figure 3-6 DLS results for the nanoparticle size (nm).

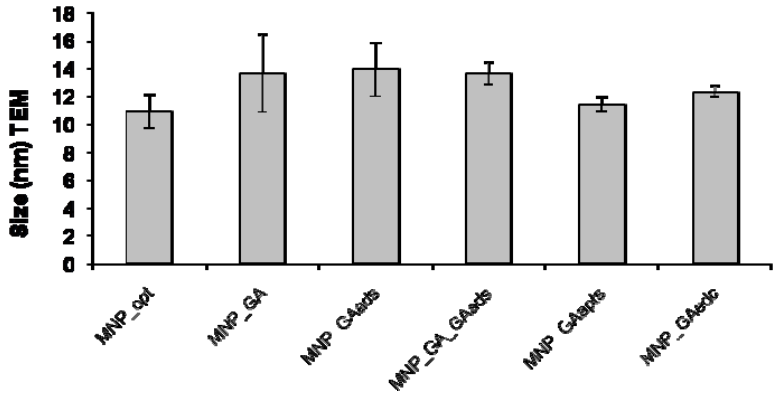

Figure 3-7 TEM results for the nanoparticle size (nm).

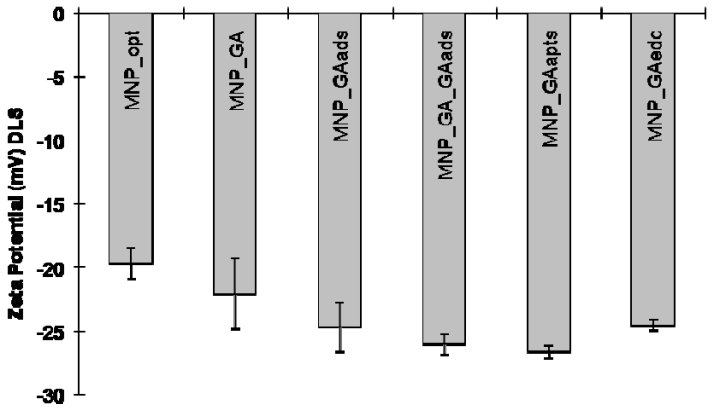

Figure 3-8 DLS results for the nanoparticle Zeta potential (mV).

FTIR spectra were generated for nanoparticles functionalized with amine groups and all the nanoparticle samples coated with GA, in order to identify the functional groups present (Table 3-4).

Table 3-4 Comparison of FTIR results obtained for surface modified nanoparticles with Gum Arabic.

MNP cm^{-1}	GA cm^{-1}	MNP_GA_GA_{ADS} cm^{-1}	MNP_GA_{ADS} cm^{-1}	MNP_GA_{APTS} cm^{-1}	MNP_GA_{EDC} cm^{-1}
3450	3450	3429 – 3450	3650	3677	3650
-	2926	2942	2928	2923	2923
2371 – 2272	2397 – 2349	2371	2361		
			1718	1772	1774
1614	1638 – 1600	1643		1600	
			1500	1490	1500
-	1424		1458		1458
		1386	1384	1384	1384
-	1032 – 1076	1043	1035 - 1065	1035 - 1072	
	977				
-		857	874		
			802	804	803
571	552	571	566	585	

From FTIR results, it can be seen GA is present at the surface of GA coated MNPs. The spectra of the coated iron oxide nanoparticles contains characteristic OH stretching (ν OH) and HOH bending (δ OH) vibrational bands at 3429 - 3450 cm^{-1} and at 3650 – 3677 cm^{-1} due to the adsorbed water in the sample. The 2923 - 2942 cm^{-1} peak is characteristic of GA stretching vibrations of the C-H bond (ν C-H of $–CH_2$) and was observed in all MNPs modified with GA. In GA the absorption band at 2361 – 2371 cm^{-1} is usually due to CO_2 vibration but this peak superimposes with a characteristic band of bare magnetite. Carboxylate groups associated with the Gum Arabic molecule show a strong peak at 1600 - 1643 cm^{-1} (C=O stretch and N-H bending) which is not visible in MNP_GA_{ADS} and MNP_GA_{EDC}, possibly due to the involvement of this species in binding to the MNP surface. Bands in the regions of 1458 and 1035 – 1072 cm^{-1} in GA modified MNPs are due to the C-O bond stretch. A ν(Fe-O) peak is observed for MNP_GA_GA_{ADS}, MNP_GA_{ADS} and MNP_GA_{APTS} samples at 571, 566 and 585 cm^{-1}

respectively [43, 57, 68, 96]. Adsorption bands for amine groups in GA, bands due to N-H stretch for primary amine (3400 - 3500 cm^{-1}) and secondary amine (3310 – 3350), have not been clearly identified in these samples. An explanation possible is that Gum Arabic is made up of a high molecular weight glycoprotein and a higher amount of a lower molecular weight polysaccharide and the adsorption bands due to the N-H stretch may be covered by the broad adsorption band at 3000 – 3600 cm^{-1} due to the O-H stretch of the polysaccharide [30, 97].

Experiments were conducted in order to ascertain the possible displacement of adsorbed or covalently coupled GA by phosphate ions when the nanoparticles are maintained in phosphate buffer. This test was performed because further tests of the MNPs in mammalian cell cultures include the use of phosphate-based buffers. The displacement studies were performed once and the results are presented in Figure 3-9.

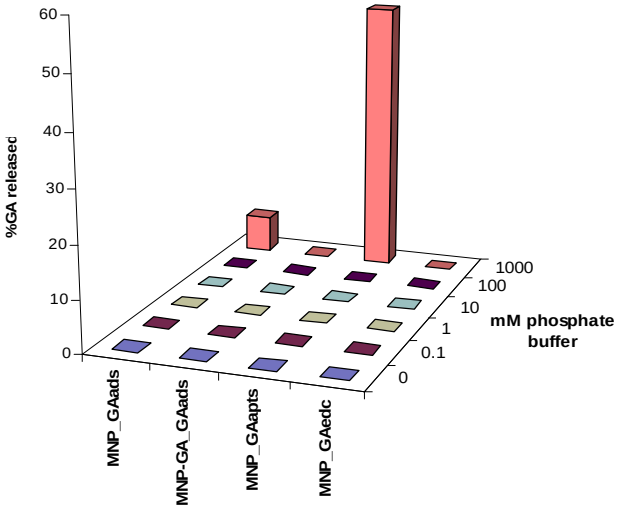

Figure 3-9 Displacement of adsorbed or covalently bound Gum Arabic on magnetic nanoparticles by different phosphate buffer solutions (n = 1).

Displacement of GA in MNP_GA_GA_{ADS} and MNP_GA_{EDC} did not occur in any of the phosphate buffer concentrations tested. MNP_GA_{ADS} and MNP_GA_{APTS} displayed 7 and 52% displacement respectively, when in contact with a 1 M phosphate buffer solution. The GA adsorption onto magnetite nanoparticles is due to the electrostatic attraction between negatively charged groups of a GA molecule and a positive site on the oxide surface. In the MNP_GA_{ADS}, when in contact with phosphate buffer solutions,

a competition for the iron oxide surface occurs between phosphate and GA. A GA displacement is then observed for the highest concentration of phosphate tested. The displacement values obtained are smaller than those reported previously for GA adsorbed at the surface of bare magnetite [28]. The displacement value of 52% for MNP_GA_{APTS} is very high and was not expected considering that GA is expected to be covalently linked to MNPs.

3.4. Conclusions

Surface modification of MNPs with GA via adsorption or covalent coupling was studied. A range of 0,8 to 2,80 g GA/g MNP was observed for the adsorption and covalent coupling of GA onto functionalized nanoparticles. The maximum of GA deposited at the MNP surface was obtained for MNP_GA_{EDC} (2,80 ± 0,00 g GA/ g MNP), followed by the maximum obtained for the MNP_GA_{ADS} (1,09 ± 0,42 g GA/ g MNP). The lowest value was observed for the MNP_GA_{APTS}.

The modified nanoparticles presented mean average sizes in the range of 11-14 nm, very similar to the values for bare magnetite (MNP)(11 ± 3 nm) and GA-co-precipitated nanoparticles (MNP_GA)(14 ± 4 nm) in Chapter 2. Agglomerates of nanoparticles were identified in all samples studied in TEM and DLS analysis; the agglomerate diameters determined were in the range of 950-2818 nm for the TEM analysis and 1120-1500 nm in the DLS measurements, the discrepancy of values was accounted for the difference of analytical method. Nanoparticle agglomerate diameters determined by TEM and DLS were very similar to the values for MNP (2652 and 1476,67 ± 135,77 nm) and MNP_GA (950 and 341,33 ± 69,06 nm) (Chapter 2).

The lower zeta potential values obtained for GA treated nanoparticles further corroborated the increase in nanoparticle dispersivity due to GA coating. Values from -22,07 to -26,63 mV were obtained for GA treated nanoparticles comparing to the -19,63 mV obtained for MNP.

FTIR peaks at 2923 - 2942 cm^{-1}, characteristic of GA stretching vibrations of the C-H bond (ν C-H of $–CH_2$), and in the region of 1458 and 1035 – 1072 cm^{-1} due to the C-O bond stretch characteristic of Gum Arabic, were identified in GA treated nanoparticles corroborating the Gum Arabic presence in these nanoparticles.

Adsorption and Covalent coupling values obtained were higher than reported previously [28] for GA adsorption onto iron oxide nanoparticles and an increase in MNP stability was observed for the surface modified nanoparticles corroborating the Gum Arabic effect in preventing further agglomeration of the nanoparticles in solution.

Chapter 4 – Studies on the Influence of Magnetic Particles on the Growth of Mammalian Cell Lines and Cellular Viability

4.1. Introduction

An important step during the development of nanoparticles that may be used for biomedical applications is to test them for biocompatibility. One possible experimental strategy is to grow mammalian cell lines in the presence of MNPs and to determine the effects that the particles may have on the cellular growth and viability. The observed effects will dictate the fate of the synthesized and surface modified nanoparticles. In case of toxic effects, the biocompatibility of the MNPs can be improved by different surface modifications. Several groups have performed cell interaction studies with nanoparticles [16, 25, 52, 56, 86, 87, 89, 90]. Recently, Wilson et al. (2008) [59], synthesized magnetite MNPs in the presence of oleylamine (OLA) or Gum Arabic (GA) and used the particles to study the effect of these surface modifications on the dispersivity of the MNPs and on the cellular level of bioactivity of L929 fibroblasts (indicated by the level of cytotoxicity). OLA modified MNPs displayed the highest level of cytotoxicity with approximately 27% of L929 fibroblast cells dead after an exposure period of 24 hours to OLA, while untreated magnetite, GA treated and cells grown in the absence of MNPs displayed only a 10% decrease in cellular density. These authors reported that untreated and OLA treated MNPs were observed in the cell cytoplasm while GA-modified MNP clusters were located at the cell membrane. They related these results to the observations that the bare magnetite and OLA modified nanoparticles exhibited the highest dispersivity values and that the MNPs with GA adsorbed onto the MNP surface formed large particle agglomerates during synthesis. Accordingly, they suggested that GA may prove useful as a coating material for the preparation of biocompatible MNPs.

In this work, bare magnetite MNPs, and particles functionalized with GA (MNP_GA_{ADS}, MNP_GA_GA_{ADS}, MNP_GA_{APTS} and MNP_GA_{EDC}) were used for *in vitro* tests with mammalian cell lines in order to determine the effects of the nanoparticle coating on cellular viability and growth, as compared to cell cultures

grown in the absence of MNPs. The tests were performed on different cell lines, namely HEK293 (*Human Embryonic Kidney cells*), TE671 (*Human Caucasian Medulloblastoma*) and CHO (*Hamster Chinese Ovary*). These assays were performed to investigate for possible common effects of the particles on cells from different origins and characteristics. HEK293 cells were the most sensitive to the presence of MNPs and were used to follow the development of the toxic effects over time. Additionally, GA coated MNPs were functionalized with the fluorophore Fluorescein isothiocyanate (FITC) and these particles were tested in the cell cultures as an attempt to determine if the particles may be internalized by the cells.

4.2. Materials and Methods

4.2.1. Materials

Gum Arabic was purchased from Sigma-Aldrich.

Trypan blue Standard stain ((3Z)-5-amino-3-[[4-[4-[(2Z)-2-(8-amino-1-oxo-3,6-disulfonaphthalen-2-ylidene)hydrazinyl]-3-methylphenyl]-2-methylphenyl]hydrazinylidene]-4-oxonaphthalene-2,7-disulfonic acid) (2704540) was purchased from The British Drug Houses LTD (BDH) Laboratory Chemicals division.

N', N'' – dimethylformamide (DMF)≥99,8% A.C.S Reagent 319937-1L Sigma-Aldrich

Ethanol Absolute PA was purchased from Panreac.

Dulbecco´s Modified Eagle Medium, Ham's F12 Medium, Foetal bovine serum, Penicillin, Streptomycin and Fungizone were purchased from Gibco.

Fluorescein isothiocyanate, Isomer I (FITC) (F7250) and Di-methil-sulfoxide (DMSO) were purchased from Sigma.

4.2.2. Equipment

Solid reagents were weighed in an Analytical Balance Sartorius BL6100.

Nanoparticle solution sonication was performed in a Bandelin Sonorex super RK25577 sonicator and nanoparticle solutions were vortexed using a Techmatic TM1 Vortex.

Incubation of nanoparticle solutions during reactions was performed in a Swinging Shaker Rotabit from P Selecta.

Fluorescence assays were performed under an Olympus Bx51 microscope (400x amplification), with Olympus Fluorescence Filters U-MWB2 and U-MWG2, an Olympus U-RFL-T lamp, an objective Uplan FL N, 40x, PH1 and PH2 and a Cell F-View Image System Software for monitoring. Photographs were taken of 6 to 10 random fields of each sample.

The Fluorescence Filter U-MWB2 (λ_{exc} = 460-490 nm, λ_{em} = 520 nm IF) was used to observe the emitted fluorescence from FITC, the Fluorescence Filter U-MWG2 (λ_{exc} = 510-550 nm, λ_{em} = 590 nm) was used to observe the Trypan Blue dye emitted fluorescence. Optical analysis of the samples was performed in Phase contrast.
Cell culture handling operations were performed in sterility inside a Sanyo laminar flow chamber.
Cell cultures were grown in a Nuare-IR CO_2 and Temperature controlled incubator.

4.2.3. Methods

The nanoparticles used for the *in vitro* assays were synthesized and further coated with GA (Chapters 2 and 3). The cell cultures were grown in the presence of bare magnetite MNPs (MNP) and GA-functionalized MNPs (MNP_GA_{ADS}, MNP_GA_GA_{ADS}, MNP_GA_{APTS} and MNP_GA_{EDC}). Cellular viability was accessed by the Trypan Blue exclusion test and by comparing the cellular density of the cultures with those grown in the absence of MNPs (control).

4.2.3.1. Functionalization of GA with FITC

Two different approaches for the FITC labeling of MNPs were tested: (A) FITC functionalization of Gum Arabic before MNP coating and (B) Gum Arabic functionalization with FITC at the surface of MNPs.

(A) Dimethylformamide (200 µl) was combined with FITC (1 mg) and the solution was added to ethanol (1 ml, 95%) to create a master solution. In a separate vial, Gum Arabic (15 ml, 40 mg/ml) was mixed with phosphate buffer saline (3 ml). An aliquot of the master solution (100 µl) was added dropwise to the Gum Arabic-PBS solution with stirring and the solution was incubated for 1 hour on a gyratory shaker.

MNPs were coated with Gum Arabic-FITC following the adsorption and covalent coupling protocols used in Chapter 3.

(B) Solutions of MNPs synthesized using Massart's Method and coated with Gum Arabic containing FITC as a fluorescent marker were prepared in Phosphate buffer saline. An aliquot of the master solution prepared in (A) (100 µl) was added dropwise to the MNPs-PBS solutions, which were then incubated for 1 hour with stirring on a gyratory shaker.

The exposition time for the photographs taken of cells in the presence of FITC was of 140 milliseconds which was the minimum time needed to observe fluorescence of the tagged particles.

4.2.3.2. Protocol for the establishment and maintenance of Cell lines

For the *in vitro* assays, three cell lines were established and maintained. HEK293 cells (*Human Embryonic Kidney cells*, ECACC No. 85120602), TE671 cells (*Human Caucasian Medulloblastoma*, ECACC No. 89071904) and CHO cells (*Hamster Chinese Ovary*, ECACC No. 85050302) were purchased from the European Collection of Cell Cultures. Cellular suspension samples were stored in aliquots in liquid nitrogen (-210ºC). After each sample was taken from the liquid nitrogen chamber, it was left at room temperature for one minute. Then the samples were put in a water-bath at 37ºC until partial thawing of cells with release from the cryotube walls was observed. Inside the laminar flow chamber the semi-thawn sample was added to different culture flasks filled with culture medium (12 ml). HEK293 and TE671 cells were grown in D-MEM culture medium (*Dulbecco´s Modified Eagle Medium*, Gibco) with 4500 mg/L glucose, +*GlutaMAX*™ *I*, without pyruvate. CHO cells were grown in F-12 medium with glutamine. All culture media were enriched with 10% foetal bovine serum and supplemented with 50 I.U/ml penicillin and 50 U.G/ml streptomycin to prevent for bacterial infections. The flasks with the cellular suspensions were placed at 37ºC in a humidified atmosphere with 5% CO_2 and 95% air. Culture media were changed as soon as the cells adhered to the substrate of the culture flasks to prevent prolonged exposure periods of the cells to di-methil-sulfoxide, present in the cryopreservation media and toxic to the cells.

Sub-culture was performed by trypsinization when cellular growth reached approximately 70% confluence. All solutions were warmed in a water-bath at 37ºC before use. The old medium was removed from each culture flask and the cells were washed with PBS (5 ml, phosphate buffered saline: 8g NaCl, 0.2g KCl, 1.44g Na_2HPO_4, 0.24g KH_2PO_4 per liter, pH 7.4, autoclaved) in order to remove the remaining serum, an inhibitor of trypsin. PBS was discarded and trypsin was added to the cell cultures (8 drops, 0.05% in EDTA.4Na) to digest the extracellular matrix. The trypsinization reaction was stopped by the addition of culture medium (3 ml) to the cells, which were further ressuspended with a Pasteur pipette. The cellular suspensions were used to propagate the cultures in new flasks with fresh culture medium.

All operations with the cells were performed under sterility conditions inside a laminar flow chamber. All materials that were in contact with cells were autoclaved before being disposed of.

4.2.3.3. *in vitro* studies of Mammalian Cell lines grown in the presence of MNPs

To prevent contamination of the cell cultures, the magnetic nanoparticles were washed 3 times with autoclaved PBS buffer supplemented with penicillin (50 I.U/ml), streptomycin (50 U.G/ml) and fungizone (2,5 μg/ml). Solutions of coated and uncoated MNPs in PBS buffer (1mg/ml) were stored at 4ºC until further use. MNP samples used for these assays were bare magnetite MNPs (MNP), GA adsorbed (MNP_GA_{ADS} and MNP_GA_GA_{ADS}), and GA covalently coupled MNPs (MNP_GA_{APTS} and MNP_GA_{EDC}). The cells for the in vitro essays with the MNPs were grown onto 13 mm diameter coverslips placed inside 35 mm diameter culture dishes.

The different MNP samples (50 μl) were added to different culture dishes with growing cells. At different times ranging from 30 minutes up to 30 hours samples were observed under the microscope. Prior to each observation a coverslip with cells was placed inside a culture disk with PBS and washed by gentle shaking for 5 mins to remove excess of articles that could mask the results. Additionally, GA (40 mg/ml) was also tested using the same protocol. The cellular density of each sample was compared to that of the cells grown in the absence of MNPs, which were used as controls.

4.2.3.4. Cell Viability Trypan Blue exclusion Test

Trypan Blue is a dye that only penetrates the cell membrane when cells are not viable, momentarily or definitely [103, 104]. Although this test is usually performed under normal optical microscopy, it was observed by our group that Trypan Blue has a λ_{exc} at 500 nm and a maximum of λ_{em} at 650nm (red) allowing for a better discrimination between viable and unviable cells when using the green filter U-MWG2. The Trypan blue test was performed in HEK293 cells and HEK293 cells incubated with MNPs or GA, to assess cell viability during the *in vitro* assays.

A coverslip with attached cells was placed in a Petri dish containing Trypan blue solution (0,0072 g Trypan Blue, 10 ml PBS buffer) for 10 minutes. Afterwards, the coverslips were washed with PBS buffer to remove excess of dye and observed under phase contrast and using the green filter U-MWG2. The exposition time chosen for the photographs taken of cells was 310 ms, which was the average exposure time set automatically by the microscope for the Trypan blue solution.

4.3. Results and Discussion

4.3.1. Assays of MNPs with different cell lines (HEK293, CHO and TE671)

In order to determine if MNPs may interact differently with cells of different proveniences, three cell lines were used for these studies. The cell lines were incubated with the nanoparticles for 24 or 30 hours and the individual samples were observed under phase contrast optical microscopy. Several MNP concentrations were tested and a 1mg/ml nanoparticle concentration was chosen as allowing for a better observation of the effects of MNP interaction with cells. Each assay was performed independently on different days and the observations from each assay were made on at least 6 random fields per sample. The results presented here are a qualitative measure of the observed effects at 24 and 30 hours and the most representative photos of each sample are presented in Figure 4-1.

For a more comprehensive analysis of the observations, Table 4-1 summarizes the information that was gathered concerning cellular density of the cultures (C), amount of

nanoparticles deposited to the surface of the cells (P) and the absence or presence of cellular debris (D), an additional indication of cellular damage.

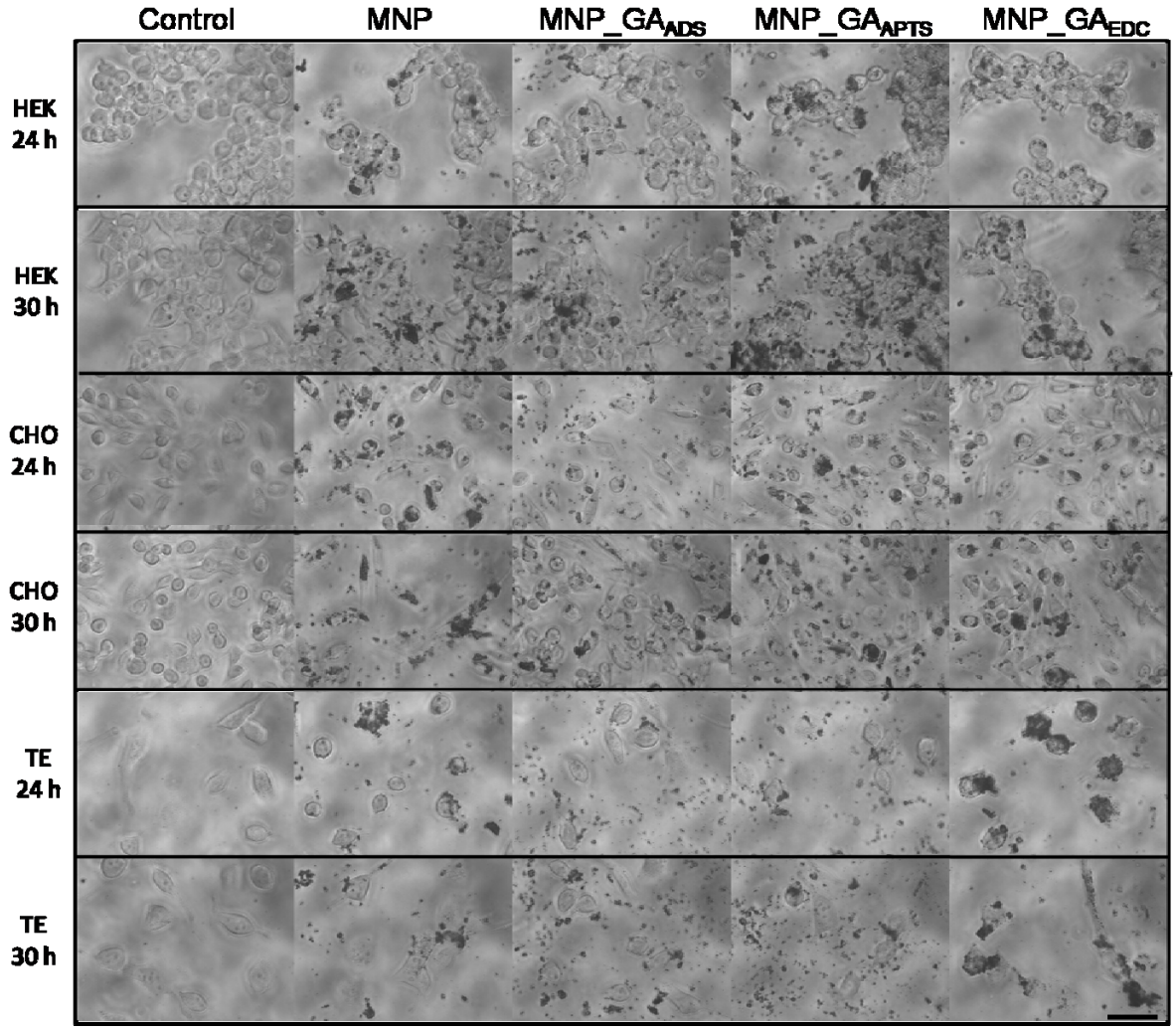

Figure 4-1 Phase contrast photographs of mammalian cell lines grown in the absence or in the presence of different MNPs. The incubation times were 24 and 30 hours (n = 5, bar represents 50 µm).

Table 4-1 Comparison of cellular density (C), presence of MNPs at the cells surface (P) and cellular debris (D) on HEK293, CHO and TE671 cell cultures, at 24 and 30 hours incubation times (n=5).

Cell line	Inc. Time (h)	Control			MNP1			MNP2			MNP3			MNP4		
		C	*P*	*D*	*C*	*P*	*D*	*C*	*P*	*D*	*C*	*P*	*D*	*C*	*P*	*D*
HEK	24	0			-	++++	0	-	++	0	-	++++	+	-	++++	+
	30	0			0	++++	+	-	+++	0	0	++++	0	-	++++	+
CHO	24	0			-	++++	+	-	++	+	-	++++	+	-	++++	+
	30	0			0	++++	+	0	+++	+	0	++++	+	-	++++	+
TE	24	0			0	+++	0	-	+	0	-	++	0	-	++++	+
	30	0			-	++	0	-	+	0	-	++	+	-	++++	+

Key: (0) no effect, (-) decrease in cell density (+) <1/4 presence of MNPs on cell surface / presence of debris, (++) ~1/4 cells with MNPs, (+++) ~½ cells with MNPs, (++++) ≥ 3/4 cells with MNPs.

All tested NMPs have the ability to deposit, and most likely attach, onto the surface of the three cell types tested, as shown in Figure 4-2.

More than 3/4 of all cells have nanoparticles attached and/or present cellular debris when grown for 24 or 30 hours in the presence of uncoated nanoparticles (MNP) or for GA covalently coated magnetic nanoparticles (MNP_GA_{APTS} and MNP_GA_{EDC}). Cells exposed to GA adsorbed onto magnetite nanoparticles (MNP_GA_{ADS}) present lower density of cells with nanoparticles attached (1/4 to ½ of the total cells for CHO and HEK cells and less than ¼ of the total cells for TE cells) than with the other MNPs.

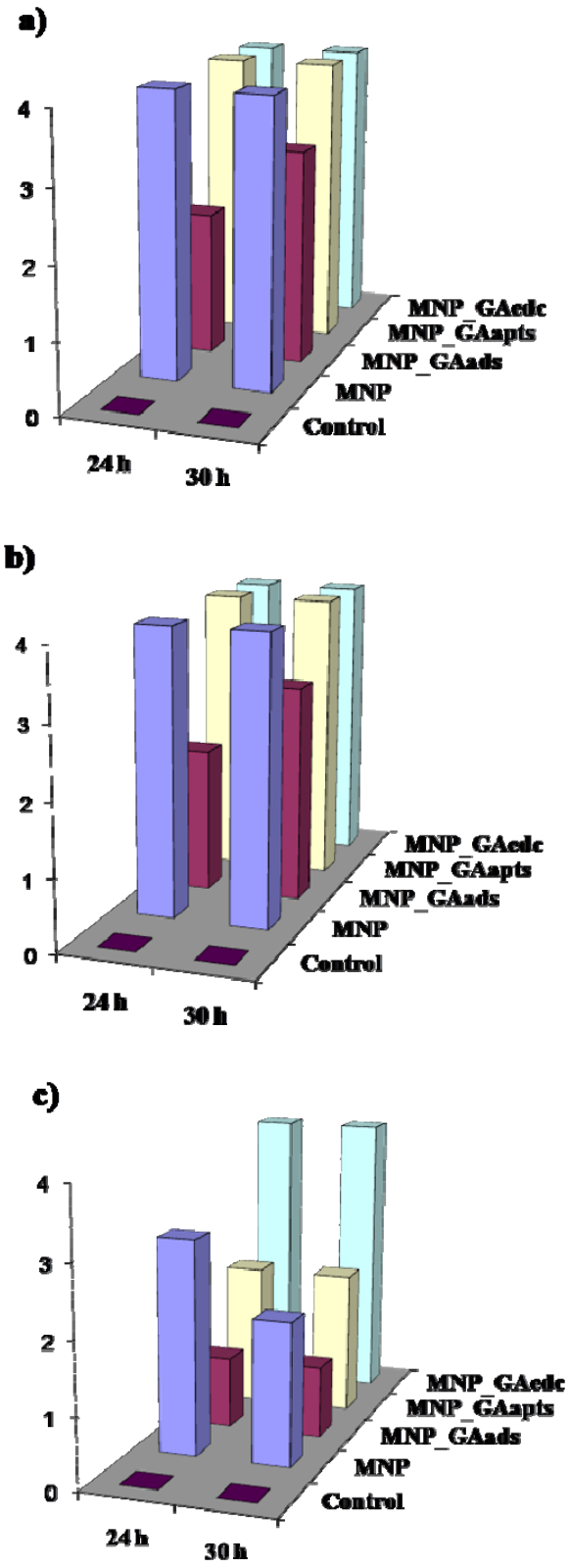

Figure 4-2 Comparison of the amount of MNPs observed at cellular surface between (a) HEK293, (b) CHO and (c) TE671 cells.

Key: (0) no effect; (1) <1/4, (2) ~1/4, (3) ½ and (4) ≥ 3/4 cells with MNPs.

On what concerns the amount of particles deposited at the surface of the cells, the behaviour of all particles is similar between HEK293 and CHO cultures (Figure 4-3). Nevertheless, the presence of cellular debris (an indication of cellular death) was mostly observed on CHO cultures. With the exception of MNP_GA_{EDC}, all other tested particles are less effective on attaching to the surface of TE671 cells when compared to the results obtained with HEK293 and CHO cells. These results show that the particles may act differently on distinct cellular types.

The GA covalently coated magnetic nanoparticles (MNP_GA_{EDC}) showed a more deleterious effect than the other MNPs. They were observed on more than ¾ of cells on all the performed assays. Their negative influence on cellular survival was also confirmed by the presence of cellular debris on all cultures and by a decrease on cellular density in comparison with the control. MNP and MNP_GA_{APTS} particles were mostly observed at the surface of HEK293 and CHO cells, which cultures also presented cellular debris.

In most situations there was a decrease in cellular density of the cultures grown in the presence of MNPs when compared to the control, an indication that the particles compromise cellular viability. Nevertheless, in some assays this was not observed and the cellular density of the cultures remained unchanged, in particular for the longer incubations (30 hours). A possible explanation is that the MNPs may attach at shorter incubation times than the ones chosen for the observations, and that the cells which were not covered by the particles had the possibility to proliferate. To address this question, further assays at shorter incubation times were performed. For these assays the HEK293 cells were chosen due to their high sensitivity to the presence of MNPs and because the group had previously developed protocols for the transfection of cDNA codifying for antibodies to be used for localization studies.

4.3.2. Assays with HEK293 cells at different incubation times (30 min to 30 hours)

Samples of HEK293 cells were grown in the presence of the different types of MNPs. After different incubation periods, which ranged from 30 minutes to 30 hours, samples of cells grown onto coverslips were observed by optical phase contrast microscopy. The results are shown in Figure 4-3. Cells grown in the absence of particles were used as control. The qualitative information gathered from the photographs taken of the

different cells concerning the amount of cells which present particles at the surface, cellular density of the cultures and presence of cellular debris is shown in a comprehensive way in Table 4-2.

For an easier understanding, the data which only concerns the amount of cells which present particles at their surface was additionally organized in the form of a tri-dimensional bar graph (Figure 4-4).

It was observed that all the particle types could adhere to the surface of the HEK293 cells after only 30 minutes of incubation. Nevertheless, different incubation periods are required to observe the same density of cells covered by the different types of MNPs tested. Factors such as the type of MNP chemical modification and the subsequent number and nature of groups at the surface of the MNPs, the size of the particles and dispersibility could underlie the observed differences. GA covalently coupled MNPs (MNP_GA_{APTS}) particles showed a faster ability to attach to the cells with ¼ of the cells are covered by MNPs after only 30 minutes. The amount of cells with MNP_GA_{APTS} attached remained stable up to 6 hours, after which the number of cells showing particles at its surface increased to more than ¾.

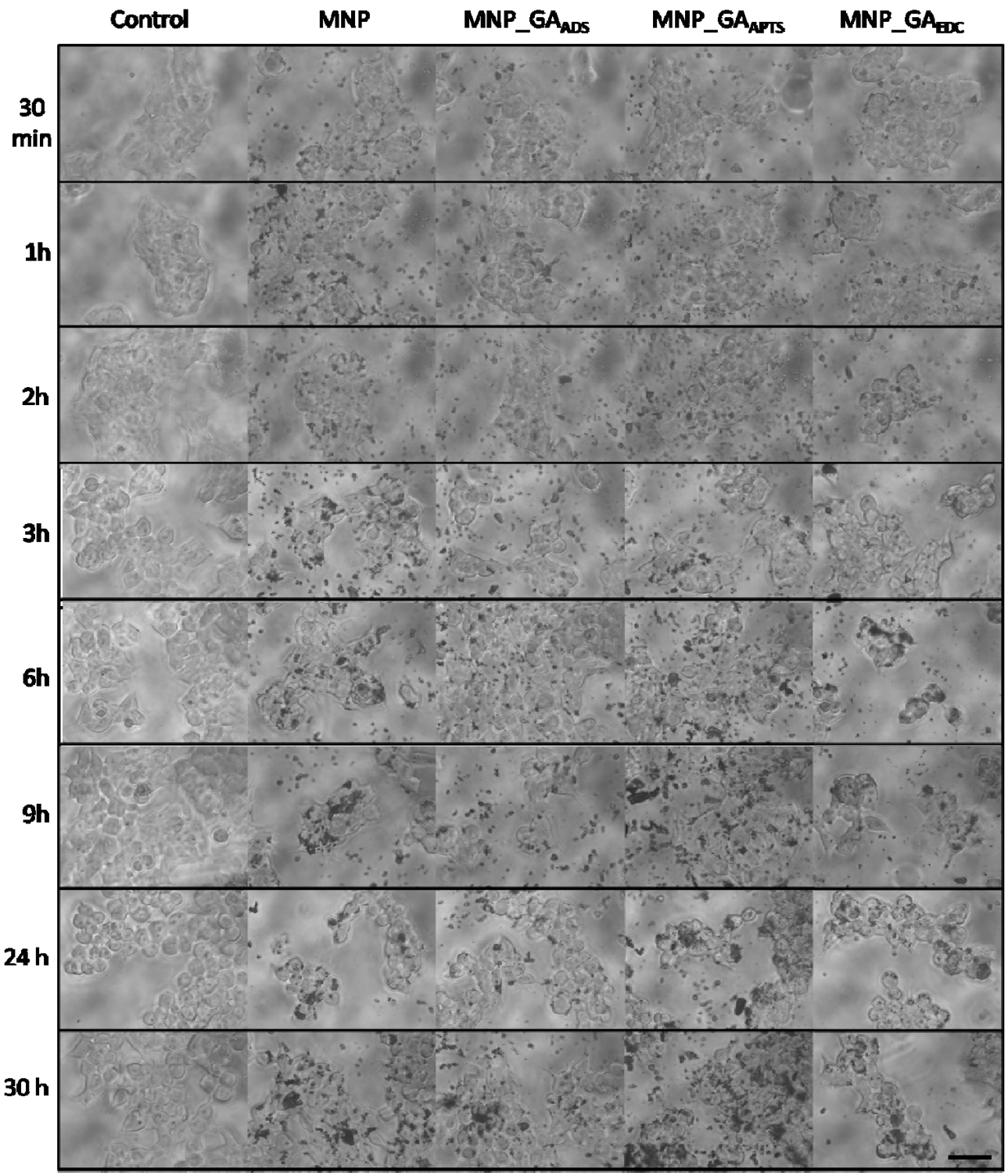

Figure 4-3 Phase contrast photographs of HEK293 cells grown in the absence or in the presence of different MNPs. The incubation times varied between 30 mins and 30 hours (30 min to 3 hrs, n = 3; 6 and 9 hrs, n = 2; 24 and 30 hrs, n = 5. bar represents 50 µm).

Table 4-2 Comparison of cellular density (C), presence of MNPs at the cells surface (P) and cellular debris (D) on HEK293 cell cultures, at different incubation times.

Cell line	Inc. Time (h)	Control			MNP			MNP_GA$_{ADS}$			MNP_GA$_{APTS}$			MNP_G$_{EDC}$		
		C	*P*	*D*	*C*	*P*	*D*	*C*	*P*	*D*	*C*	*P*	*D*	*C*	*P*	*D*
Hek 293	0,5	0			0	+	-	0	+	-	0	++	-	0	+	-
	1	0			0	+++	-	0	+	-	0	++	-	0	++	-
	2	+			0	+++	-	0	+	-	0	++	-	0	+++	-
	3	+			0	+++	-	0	+	-	0	++	-	-	+++	+
	6	+			-	++++	-	0	+	-	0	++	-	-	++++	+
	9	+			-	++++	-	-	+	-	-	++++	-	-	++++	+
	24	0			-	++++	-	-	++	-	-	++++	+	-	++++	+
	30	0			0	++++	+	-	+++	-	0	++++	-	-	++++	+

Key: (0) no effect, (-) decrease in cellular density / absence of cellular debris, (+) <1/4 presence of MNPs on cell surface / presence of debris, (++) ~1/4 cells with MNPs, (+++) ~½ cells with MNPs, (++++) ≥ 3/4 cells with MNPs.

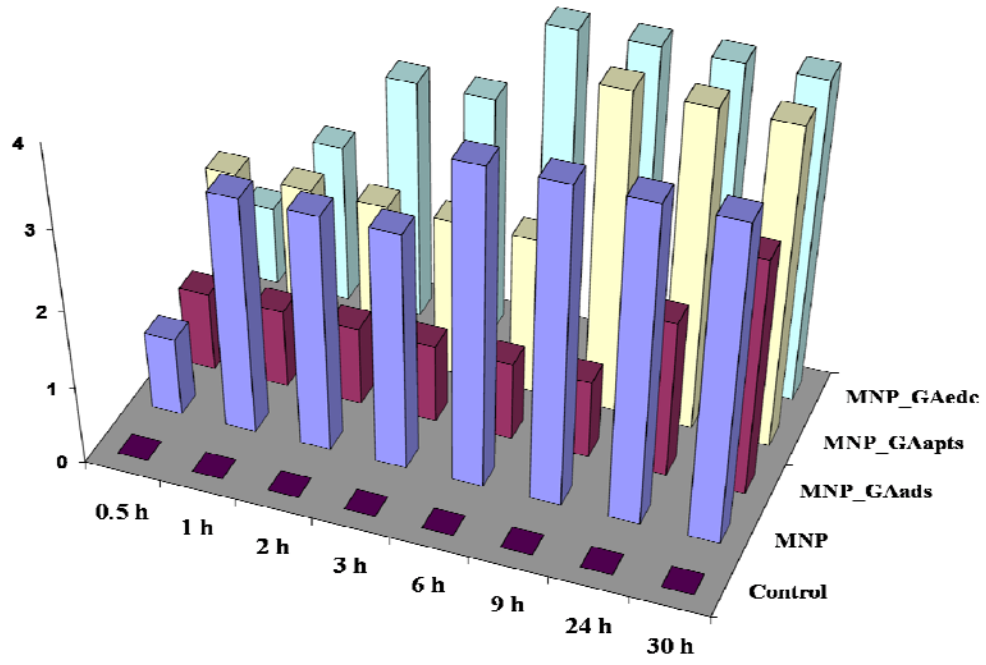

Figure 4-4 Comparison of the amount of MNPs observed at cellular surface of HEK293 cells at different incubation times.

Key: (0) no effect; (1) <1/4, (2) ~1/4, (3) ½ and (4) ≥ 3/4 cells with MNPs.

Bare magnetite (MNP) and GA covalently coupled MNPs (MNP_GA_{EDC}) displayed relatively similar behaviour, with less than ¼ of the cells with MNPs after 30 minutes of incubation, followed by a rapid increase to ½ between 1 and 3 hours, and more than ¾ of the cells already at 6 hours incubations periods. The results with HEK293 cells confirm the previous results obtained from the three mammalian cell lines showing that MNPs coated with adsorbed GA (MNP_GA_{ADS}) are the less effective particles on attaching to the cells, accounting for less than ¼ of cells with the MNPs at their surface up to 9 hours of incubation. After 6 hours in the presence of particles, all samples tested presented values higher than 3/4 of cells with particles, except for those with MNP_GA_{ADS}. The work of Wilson et al. (2008) [59] had already showed that MNPs treated with GA caused only 10% of decrease in cellular density of L929 fibroblasts. Nevertheless, these authors showed that bare magnetite had a similar effect to the coated particles, which contradicts our results with HEK293, CHO and TE671 cells. It is possible that the difference is due to the characteristics of the cell lines used. These authors also synthesized the particles in presence of GA, while for the preparation of MNP_GA_{ADS} GA was adsorbed to the particles. They incubated the cells overnight in the presence of particles. It is possible that the cells which did not presented particles may have also multiplied during the incubation period, changing the results. This was observed in some of our assays.

The level of cellular viability observed seems to follow the proportion of cells with particles for corresponding incubation periods. This was assessed by a decrease in the number of cells per sample (when compared to the control) and/or by the presence of cellular debris (Figure 4-3, Table 4-2 and Figure 4-4). In general, samples showing higher amounts of cells with particles attached also showed a decrease in cellular density, possibly due to the release of dead cells during the washing procedure with PBS. Accordingly, the cellular density of the cultures decreased after 3 hours (MNP_GA_{EDC}), 6 hours (MNP) and 9 hours (MNP_GA_{APTS} and MNP_GA_{ADS}).

Another indicator of cellular inviability was the observation of cellular debris attached onto the coverslips. These were particularly evident in samples of HEK293 cells grown in the presence of MNP_GA_{EDC} for periods longer than 3 hours, inclusive. As to the other samples, debris were only observed for incubation times of 30 hours (MNP), 24 hours (MNP_GA_{APTS}) and they were never observed in those cell samples incubated

with MNP_GA_{ADS}. These results suggest that MNP_GA_{EDC} may act upon the cells by a unique mechanism.

4.3.3. Trypan Blue exclusion test for cellular viability

A Trypan Blue test was performed on HEK cells incubated with GA after 24 hours, in order to qualitatively assess if the cell viability is compromised by the cell interaction with GA itself. Cells grown in the absence of GA were used as controls (Figure 4-5).

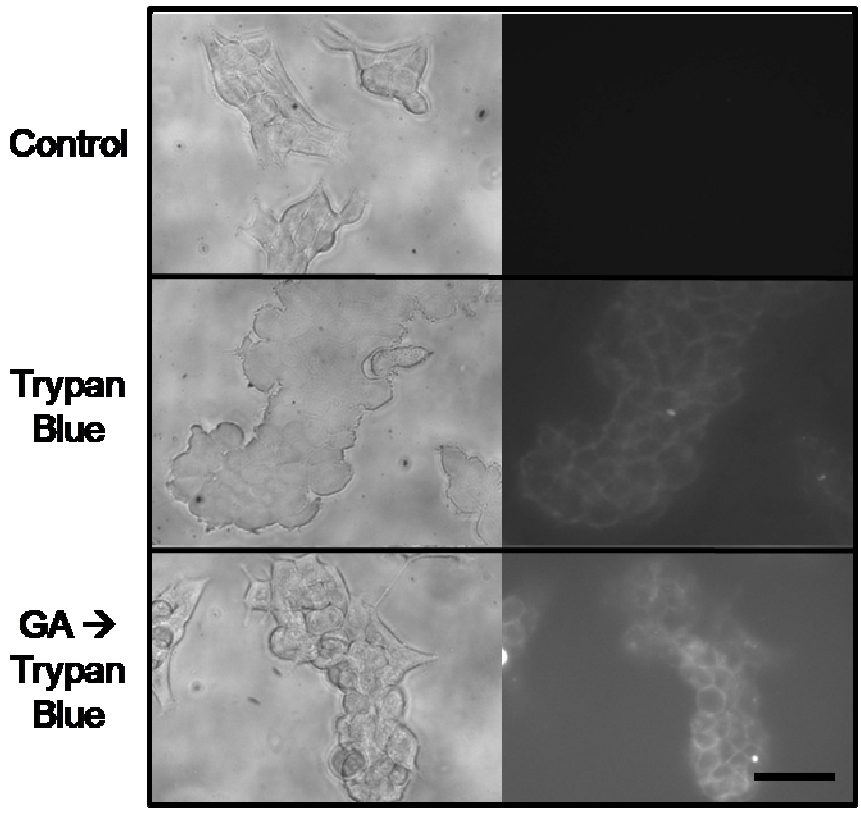

Figure 4-5 Phase contrast (left) and fluorescence microscopy photographs (right) of cells grown for 24 hrs in the absence or presence of GA. (n=1, bar represents 50 µm).

HEK293 cells *per se* do not present fluorescence (upper panel). In the absence (middle panel) and presence of GA (lower panel), Trypan blue did not enter the cells after a 10 min period incubation. This experiment shows that GA does not compromise cellular viability. In addition, the cellular density of the cultures was not affected in the presence of GA. The fluorescence photographs were taken with exposure periods of 310 ms, the time necessary for the observation of the dye alone.

The Trypan Blue test was also used to investigate the cellular viability of the cultures under the different experimental situations tested, with bare and GA-coated MNPs. The results obtained for the Trypan blue test on HEK293 cells incubated for 24 hours with the different MNPs are presented in Figure 4-6.

HEK293 cultures incubated with MNP and MNP_GA_{EDC} nanoparticles show some cells fully fluorescent, an indication of disruption of cellular integrity. These results are in accordance to those presented in Table 4-2. Cells from cultures grown in the absence of particles or in the presence of MNP_GA_{ADS} or MNP_GA_{APTS} only present fluorescence at the surface, but not inside the cells. The apparent higher level of the MNP_GA_{ADS} sample is due to the search for fluorescence performed by the microscope software leading to an overrating of the real fluorescence of the samples.

4.3.4. Localization studies of MNPs

To determine if the MNPs which are observed at the cell surface are internalized by the cells, MNPs were tagged with the fluorophore FITC (4.2.3.1). GA was also tagged to determine if it may, by itself, be internalized by the cells. When observed under the microscope, the samples of marked GA and MNPs showed different degrees of fluorescence. HEK cells were grown in the presence of GA-FITC and MNPs tagged with FITC for periods of 24 hours (MNP_GA_{ADS}-FITC, MNP_GA_GA_{ADS}-FITC MNP_GA_{APTS}-FITC and MNP_GA_{EDC}-FITC). The samples were treated as before (4.2.3.3). Nevertheless, no fluorescence was observed, nor at the surface nor inside the cells. A likely explanation for the absence of fluorescence is that for these assays a greater amount of particles is needed. Another possibility is that the fluorophore may have gone through any modification during the incubation with the cells due to the presence of the culture media.

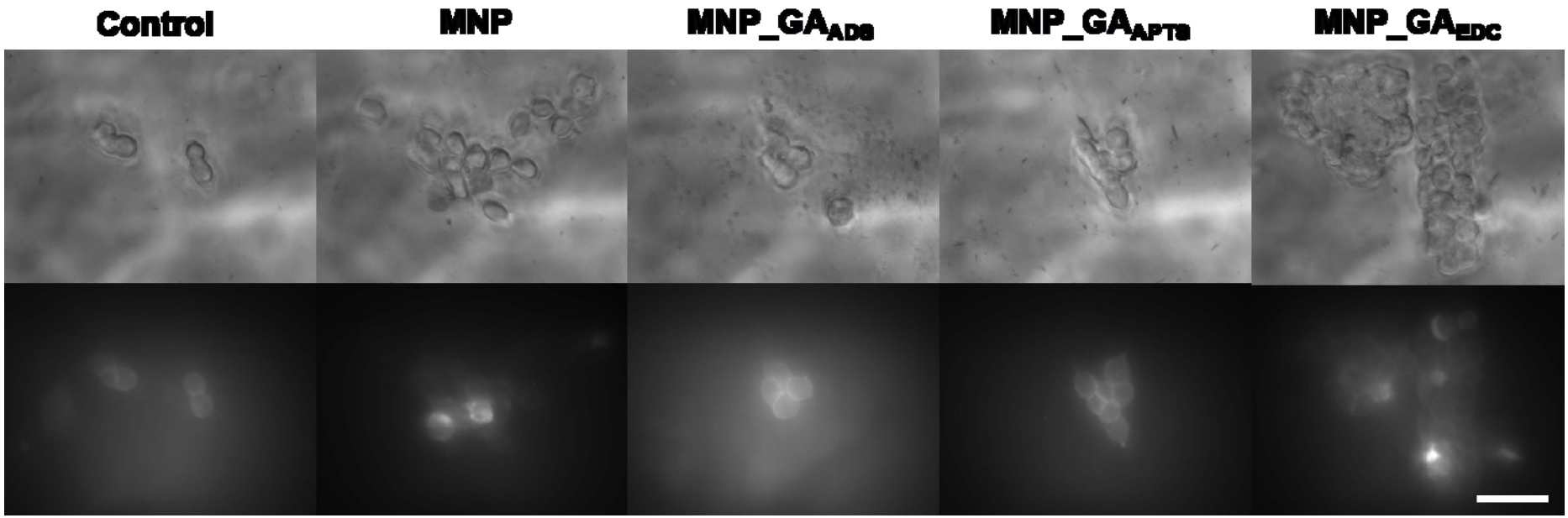

Figure 4-6 Phase contrast (upper panel) and fluorescence microscopy photographs (bottom pannel) of cells grown for 24 hrs in the absence or presence of MNPs. (n=1, bar represents 50 µm)

4.4. Conclusions

Bare magnetite (MNP) and coated MNPs were used for in vitro assays to investigate if different coatings could change the behaviour of the MNPs in contact with mammalian cell lines. The parameters followed were the density of the cell cultures (in comparison with cells grown in the absence of particles), the amount of particles at the cells' surface and of cellular debris. The trypan blue exclusion test was used to assess cellular viability.

As a first approach, assays were performed with three different cell lines (HEK293, CHO and TE671) which were incubated with the MNPs for 24 or 30 hours. All NMPs tested (MNP, MNP_GA_{ADS}, MNP_GA_{APTS} and MNP_GA_{EDC}) attached to the cell surface. In general, the amount of particles deposited at the cellular surface was high (≥ 3/4) and similar in HEK293 and CHO cultures, while TE671 cells showed lower levels of MNPs at their surface for the same incubation periods with the exception of MNP_GA_{EDC}. These particles also caused a decrease in cellular density and the occurrence of cellular debris in all samples tested. The results showed that the particles may act differently on distinct cellular types.

The HEK293 cell cultures were chosen for further assays due to their high sensitivity to the presence of the MNPs. The incubations periods of the cells with the particles ranged from 30 minutes to 30 hrs and showed different patterns of binding for the different MNPs. All particles could attach to the HEK293 cells after 30 minutes and the follow up was different for each MNP type. MNP_GA_{ADS} were the less effective on attaching to the cells, with less than ¼ of cells showing MNPs at their surface up to 9 hours of incubation. MNP_GA_{APTS} interaction with cells displayed two different stages. At an initial time of 30 minutes, MNP_GA_{APTS} nanoparticles display a higher initial interaction (more than one-fourth of the cells with nanoparticles attached), maintained stable after 6 hours of incubation. The second stage between 9 and 30 hours displayed an increase in nanoparticle attachment with more than three quarters of the cells presenting nanoparticles attached. Uncoated magnetite (MNP) and MNP_GA_{EDC} displayed a similar behaviour throughout the assays: at 1-3 hours of incubation already one half of the cells present nanoparticles attached, and from 6 to 30 hours an increase to almost all cells containing nanoparticles is observed. In all assays performed, a

decrease in cell density was observed and attributed to nanoparticle deposition and interaction with cells. This interaction with cells may probably compromise cellular viability explaining the decrease in cell density, the formation of cellular debris and the presence of unattached dead cells in the sample. In general, for all MNPs tested, the level of cellular viability followed the proportion of cells with particles.

MNP_GA_{APTS} have a greater ability to attach to the cells at the shortest incubation periods tested, but MNP and MNP_GA_{EDC} cause the greatest damage in terms of cellular viability, as demonstrated also by the Trypan Blue exclusion test. These differences may indicate the possibility of different mechanisms by which the particles interact with the cells. MNP_GA_{ADS} particles, nanoparticles with GA adsorbed, also produced less damage in the cell cultures: they require longer periods to attach to the surface of the cells, thus affecting the cellular density at longer periods than MNP and MNP_GA_{EDC}, and not causing the formation of cellular debris. The presence of GA seems to have improved the MNPs biocompatibility. By itself it does not affect the viability of the cultures.

To investigate if the particles can be internalized by the cells, the GA-functionalized MNPs were tagged with the fluorescent dye FITC. Although the marked MNPs analyzed under fluorescence microscopy showed fluorescence, no fluorescence was observed when they were incubated with cells. This assay must be repeated in the presence of a higher concentration of particles.

Chapter 5 – Concluding Remarks

The major aim of this work was to investigate if Gum Arabic (GA) - a biopolymer constituted of protein and polysaccharides - could be used to functionalize magnetite nanoparticles (MNPs) in order to increase their biocompatibility.

Magnetic nanoparticles (MNP) with an average diameter of 11 nm, as obtained by TEM, were synthesized by chemical co-precipitation in the absence and in the presence of GA. These particles were further functionalized with GA by adsorption (MNP_GA_{ADS} and MNP_GA_GA_{ADS}) or by covalent coupling (MNP_GA_{APTS} and MNP_GA_{EDC}). The modified particles presented mean average sizes of 11-14 nm. TEM and DLS analysis showed that all MNPs can form agglomerates in aqueous solutions, which are two orders of magnitude greater than the individual particles, when the solutions were settled to rest for periods of days. The presence of GA increased the dispersibility of the samples, as shown by the lower zeta potential values obtained for GA treated MNPs (-27 to -22 mV) when compared to the -19 mV for the bare magnetite nanoparticles (MNP).

The biocompatibility of the different types of particles was investigated by growing mammalian cell lines in the presence of the particles. The amount of cells with MNPs at their surface after different incubation periods was followed. It was investigated if the presence of the particles decreased the cellular density of the cultures or induced the appearance of cellular debris, which are indicators of cellular death. Additionally, the Trypan Blue exclusion test was also performed to evaluate cellular viability.

The in vitro assays performed on three cell lines (HEK293, CHO and TE671) showed that all particles can attach to the cellular surface and may act differently on distinct cell types. In particular, TE671 cells presented lower levels of particles at their surface when compared to the other cell lines.

Additionally, HEK293 cell cultures were incubated in the presence of particles for periods of 30 minutes up to 30 hours. All particle types could attach to the cells after only 30 minutes and the follow up was different for each MNP type, suggesting that the

MNPs interact with the cellular surface by different mechanisms. For the longer incubations periods, it was observed a decrease in cellular density, which was attributed to the higher amount of particles deposited at the surface of the cells. MNP_GA_{APTS} have a greater ability to attach to the cells at the shortest incubation periods tested, but MNP and MNP_GA_{EDC} caused the greatest damage in terms of cellular viability. MNP_GA_{ADS} required longer incubation periods to attach to the surface of the cells and to decrease the density of the cultures.

The future work will include the localization of the MNPs to determine if the cells have the capacity to internalize the particles or if they only deposit at the surface. This will be made by means of fluorescence microscopy on FITC-labeled MNPs and, if possible, by TEM of cells that were incubated with the MNPs. It is also planned to functionalize the particles with antibodies for specific cell membrane antigens to be used in recognition assays.

Chapter 6 – Bibliography

1. Taniguchi, N., *On the Basic Concept of Nano-Technology.* Proc. Intl. Conf. Prod. London, Part II. British Society of Precision Engineering, 1974.
2. http://www.nano.gov/.
3. Strable, E., et al., *Synthesis and characterization of soluble iron oxide-dendrimer composites.* Chemistry of Materials, 2001. **13**(6): p. 2201-2209.
4. Allison, R.R., et al., *Bio-nanotechnology and photodynamic therapy-state of the art review.* Photodiagnosis and photodynamic therapy, 2008. **5**: p. 19-28.
5. Barathur, R., et al., *New disc-based technologies for diagnostic and research applications.* Psychiatr. Genet., 2002. **12**: p. 193-206.
6. Gourley, P.I., *Brief overview of BioMicroNano technologies.* Biotechnol. Prog., 2005. **21**: p. 2-10.
7. Gupta, A.K. and A.S.G. Curtis, *Surface modified superparamagnetic nanoparticles for drug delivery: interaction studies with human fibroblasts in culture.* J Mater Sci Mater Med, 2004. **15**(4): p. 493-496.
8. Kouassi, K.G., et al., *Aptamer-Mediated Magnetic and Gold-Coated Magnetic Nanoparticles as Detection Assay for Prion Protein Assessment.* Biotechnology progress, 2007. **23**(5): p. 1239-1244.
9. Niu, F., et al., *Promotion of organic reactions by interfacial hydrogen bonds on hydroxyl group rich nano-solids.* Chem. Commun., 2008: p. 2803-2805.
10. Jain, T.K., et al., *Magnetic nanoparticles with dual functional properties: Drug delivery and magnetic resonance imaging.* Biomaterials, 2008. **29**: p. 4012-4021.
11. Nasongkla, N., et al., *Multifunctional Polymeric Micelles as Cancer-Targeted, MRI-Ultrasensitive Drug Delivery Systems.* Nano Letters, 2006. **6**(11): p. 2427-2430.
12. King, C.P., et al., *Molecular Imaging Applications in Nanomedicine.* Biomedical Microdevices, 2004. **6**(2): p. 113-116.
13. Labhasetwar, V., et al., *Iron Oxide Nanoparticles for Sustained Delivery of AnticancerAgents.* Molecular Pharmaceutics, 2005. **2**(3): p. 194-205.
14. Olsen, D., et al., *Recombinant collagen and gelatin for drug delivery.* Adv drug deliv rev, 2003. **55**(12): p. 1547-1567.

15. Berry, C.C. and A.S.G. Curtis, *Functionalization of magnetic nanoparticles for applications in biomedicine.* J Phys D: Appl Phys, 2003. **36**: p. R198-206.
16. Gupta, A.K. and S. Wells, *Surface modified superparamagnetic nanoparticles for drug delivery: preparation, characterization and cytotoxicity studies.* IEEE Trans. Nanobiosci, 2004. **3**(1): p. 66-73.
17. Ito, A., et al., *Medical Applications of Functionalized Magnetic Nanoparticles.* Journal of Bioscience and Bioengineering, 2005. **100**(1): p. 1-11.
18. Tartaj, P., et al., *The preparation of magnetic nanoparticles for applications in biomedicine.* J. Phys. D: Appl. Phys, 2003. **36**: p. R182.
19. Gupta, A.K. and M. Gupta, *Synthesis and surface engineering of iron oxide nanoparticles for biomedical applications.* Biomaterials, 2005. **26**: p. 3995 - 4021.
20. Berry, C.C., *Possible exploitation of magnetic nanoparticle-cell interaction for biomedical applications.* Journal of Materials Chemistry, 2005. **15**: p. 543-547.
21. Huber, D.L., *Synthesis, properties and applications of iron nanoparticles.* Small, 2005. **1**(5): p. 458-501.
22. Heath, J.R. and M.E. Davis, *Nanotechnology and cancer.* Annu. Rev. Med., 2008. **59**: p. 251-265.
23. Liem, K.P., R.J. Mart, and S.J. Webb, *Magnetic Assembly and Patterning of Vesicle/Nanoparticle Aggregates.* Journal of the American Chemical Society, 2007. **129**(40): p. 12080-1.
24. Cui, R., et al., *Gold nanoparticle-colloidal carbon nanosphere hybrid material: preparation, characterization, and application for an amplified electrochemical immunoassay.* Advanced functional materials, 2008. **18**: p. 1-8.
25. Neumaier, C.E., et al., *MR and iron magnetic nanoparticles. Imaging opportunities in preclinical and translational research.* Tumori, 2008. **94**: p. 226-233.
26. Williams, D.N., et al., *Magnetic Nanoparticle Mediated Gene and Cell Delivery.* Molecular Therapy, 2005. **11**((Supplement 1)).
27. Yellen, B.B., et al., *Nanoparticle Mediated Gene Delivery to Magnetized Implants.* Molecular Therapy, 2005. **11**((Suplement 1)).
28. Roque, A.C.A. and O.C.J. Wilson, *Adsorption of gum arabic on bioceramic nanoparticles.* Materials Science & Engineering C, 2007.

29. Emerich, D.F. and C.G. Thanos, *The pinpoint promise of nanoparticle-based drud delivery and molecular diagnosis.* Biomolecular Engineering, 2006. **23**: p. 171-184.
30. Banerjee, S.S. and D. Chen, *Fast Removal of copper ions by gum Arabic modified magnetic nano-adsorbent.* Journal of Hazardous Materials, 2007. **147**: p. 792 - 799.
31. Macdonald, J.E. and J.G.C. Veinot, *Removal of residual metal catalysts with iron/iron oxide nanoparticles from coordinating environments.* Langmuir, 2008. **24**: p. 7169-7177.
32. Shao, D., et al., *Monodispersed magnetite/silica composite microspheres:preparation and application for plasmid DNA purification.* Colloids and surfaces A: physicochem. Eng. Aspects, 2008. **322**: p. 61-65.
33. Mohapatra, S., et al., *Design of superparamagnetic iron oxide nanoparticle for purification of recombinant proteins.* Journal of Nanoscience and Nanotechnology, 2007. **7**(9): p. 3193-3199.
34. Liu, H.L., et al., *Synthesis of streptavidin-FITC-conjugated core-shell Fe3O4-Au nanocrystals and their application for the purification of CD4+ lymphocytes.* Biomaterials, 2008. **29**(29): p. 4003-4011.
35. Yong, Y., et al., *Preparation and application of polymer-grafted magnetic nanoparticles for lipase immobilization.* Journal of magnetism and magnetic materials, 2008. **320**: p. 2350-2355.
36. Liu, X., et al., *Synthesis of amino-silane modified superparamagnetic silica supports and their use for protein immobilization.* Colloids and Surfaces A: Physicochemical and Engineering Aspects, 2004. **238**(1-3): p. 127-131.
37. Das, M., et al., *Bio-functionalization of magnetite nanoparticles using an aminophosphonic acid coupling agent: new, ultradispersed, iron-oxide folate nanoconjugates for cancer-specific targeting.* Nanotechnology, 2008. **19**(41).
38. Massart, R., *Preparation of aqueous magnetic liquids in alkaline and acidic media.* IEEE Trans. Magn., 1981. **17**(2): p. 1247-1248.
39. Qu, S., et al., *Magnetite nanoparticles prepared by precipitation from partially reduced ferric chloride aqueous solutions.* Journal of colloid and interface science, 1999. **215**: p. 190-192.

40. Neouze, M.-A. and U. Schubert, *Surface modification and functionalization of metal and metal oxide nanoparticles by organic ligands.* Monatsh Chem, 2008. **139**: p. 183-195.
41. Del Campo, A., et al., *Multifunctional magnetite and silica-magnetite nanoparticles: Synthesis,surface activation and applications in life sciences.* Journal of Magnetism and Magnetic Materials, 2005. **293**: p. 33-40.
42. Ma, M., et al., *Preparation and characterization of magnetite nanoparticles coated by amino silane.* Colloids and Surfaces A: Physicochemical and Engineering Aspects, 2003. **212**(2-3): p. 219-226.
43. De Palma, R., et al., *Silane Ligand Exchange to Make Hydrophobic Superparamagnetic Nanoparticles Water-Dispersible.* Chemistry of Materials, 2007. **19**(7): p. 1821-1831.
44. Kim, D.K., et al., *Synthesis and characterization of surfactant-coated superparamagnetic monodispersed iron oxide nanoparticles.* Journal of magnetism and magnetic materials, 2001. **225**: p. 30-36.
45. Teng, X. and H. Yang, *Effects of surfactants and synthetic conditions on the sizes and self-assembly of monodisperse iron oxide nanoparticles.* Journal of materials chemistry, 2004. **14**: p. 774-779.
46. Kommareddi, N.S., et al., *Synthesis of superparamagnetic polymer-ferrite composites using surfactant microstructures.* Chem. Mater., 1996. **8**: p. 801-809.
47. Prozorov, T., et al., *Effect of surfactant concentration on the size of coated ferromagnetic nanoparticles.* Thin solid films, 1999. **340**: p. 189-193.
48. Kannan, R. and K.V. Katti, *Gum Arabic as a phytochemical construct for the stabilization of gold nanoparticles: in vivo pharmacokinetics and X-ray-contrast-imaging studies.* Small, 2007. **3**(2): p. 333-341.
49. Storm, G., et al., *Surface modification of nanoparticlesto oppose uptake by the mononuclear phagocyte system.* Advanced Drug Delivery Reviews, 1995. **17**: p. 31-48.
50. Ruiz, J.M. and J.P. Benoit, *In vivo peptide release from poly(lactic-co-glycolic acid) copolymer 50/50 microspheres.* J. Cont. Rel., 1991. **16**: p. 177-186.
51. Dobson, P.J. and A. Bumb, *Synthesis and characterization of ultra-small superparamagnetic iron oxide nanoparticles thinly coated with silica.* Nanotechnology, 2008. **19**: p. 335601.

52. Sasaki, T., et al., *Magnetic nanoparticles for improving cell invasion in tissue engineering.* Journal of Biomedical Materials Research Part A, 2008. **86 A**(4): p. 969-978.

53. Khor, E. and L.Y. Lim, *Implantable applications of chitin and chitosan.* Biomaterials, 2003. **24**(13): p. 2339-2349.

54. Philipse, A.P., M.P.V. Bruggen, and C. Pathmamanoharan, *Magnetic silica dispersions: preparation and stability of surface-modified silica particles with paramagnetic core.* 1994. **10**: p. 92-99.

55. Hatton, T.A. and M. Lattuada, *Functionalization of Monodisperse Magnetic Nanoparticles.* Langmuir, 2007. **23**: p. 2158-2168.

56. Zhang, Y., N. Kohler, and M. Zhang, *Surface modification of superparamagnetic magnetite nanoparticles and their intracellular uptake.* Biomaterials, 2002. **23**: p. 1553-1561.

57. Predoi, D., *A study on iron oxide nanoparticles coated with dextrin obtained by coprecipitation.* Digest Journal of Nanomaterials and Biostructures, 2007. **2**(1): p. 169-173.

58. Sahoo, Y., et al., *Alkyl phosphonate/phosphate coating on magnetic nanoparticles: a comparison with fatty acids.* Langmuir, 2001. **17**: p. 7907-7911.

59. Wilson Jr., O.C., et al., *Surface modification of magnetic nanoparticles with oleylamine and Gum Arabic.* Materials Science and Engineering C, 2008. **28**: p. 438 - 442.

60. Banerjee, S.S. and D.-H. Chen, *Glucose-grafted gum Arabic modified magnetic nanoparticles: preparation and specific interaction with concanavalin A.* Chem. Mater., 2007. **19**: p. 3667-3672.

61. Bandyopadhaya, R., O. Regev, and R. Yerushalmi-Rozen, *Stabilization of individual carbon nanotubes in aqueous solutions.* Nano Letters, 2002. **2**(1): p. 25-28.

62. Williams, D.N., et al., *Surface modification of magnetic nanoparticles using gum arabic.* Journal of Nanoparticle Research, 2006. **8**: p. 749-753.

63. Lewin, M., et al., *Tat-peptide derivated magnetic nanoparticles allow in vivo tracking and recovery of progenitor cells.* Nat. Biotechnol., 2000. **18**: p. 410-414.

64. Bhadriraju, K. and L.K. Hansen, *Hepatocyte adhesion, growth and differentiated function on rgd-containing proteins.* Biomaterials, 2000. **21**(3): p. 267-272.
65. Denizot, B., et al., *Phosphorilcoline coating of iron oxide nanoparticles.* Journal of Colloid and Interface Science, 1999. **209**(1): p. 66-71.
66. Ye, J., et al., *Surface morphology changes on silica-coated gold colloids.* Colloids and surfaces A: physicochem. Eng. Aspects, 2008. **322**: p. 225-233.
67. Burugapalli, K., V. Koul, and A.K. Dinda, *Effect of composition of interpenetrating polymer network hydrogels based on poly(acrylic acid) and gelatine on tissue response: a quantitative in vivo study.* Journal of Biomedical Materials Research, 2004. **68 A**(2): p. 210-218.
68. Predoi, D., et al., *Study of FexOy-SiO2 Nanoparticles obtained by sol-gel Synthesis.* Digest Journal of Nanomaterials and Biostructures, 2006. **1**(3): p. 93-97.
69. Chen, G. and A.S. Hoffman, *Preparation and properties of thermo-reversible, phaseseparating enzyme - oligo(N-isopropylacrylamide)conjugates.* Bioconjug. Chem., 1993. **4**(6): p. 509-514.
70. Shan, G.B., et al., *Immobilization of pseudomonas delafieldii with magnetic polyvinyl alcohol beads and its applications in biodesulfurization.* Biotechnol. Let., 2003. **25**(23): p. 1977-1981.
71. D' Souza, A.J., R.L. Schowen, and E.M. Top, *Polyvinylpyrrolidone-drug conjugate: synthesis and release mechanism.* J. Cont. Rel., 2004. **94**(1): p. 91-100.
72. Johnson, W., *Final Report of the Safety Assessment of Acacia Catechu Gum, Acacia Concinna Fruit Extract, Acacia Dealbata Leaf Extract, Acacia Dealbata Leaf Wax, Acacia Decurrens Extract, Acacia Farnesiana Extract, Acacia Farnesiana Flower Wax, Acacia Farnesiana Gum, Acacia Senegal Extract, Acacia Senegal Gum, and Acacia Senegal Gum Extract.* International Journal of Toxicology, 2005. **24**(3): p. 75 -118.
73. Islam, A.M., et al., *A review of recent developments on the regulatory, structural, and functional aspects of gum arabic.* Food Hydrocolloids, 1997. **11**(4): p. 493-505.
74. Dickinson, E., *Hydrocolloids at interfaces and the influence on the properties of dispersed systems.* Food hydrocolloids, 2003. **17**: p. 25-39.

75. Ray, A.K., et al., *Functionality of gum Arabic: fractionation, characterization, and evaluation of gum fractions in citrus oil emulsions and model beverages.* Food hydrocolloids, 1995. **9**(2): p. 123-131.
76. Tischer, C.A., P.A.J. Gorin, and M. Iacomini, *The free reducing oligosaccharides of gum Arabic: aids for structural assignments in the polysaccharide.* Carbohydrate polymers, 2002. **47**: p. 151-158.
77. Ali, B.H., A. Ziada, and G. Blunden, *Biological effects of gum arabic: A review of some recent research.* Food and Chemical Toxicology, 2008.
78. Yoon, T.H., et al., *Biocompatible Quantum Dot Nanocolloids Stabilized by Gum Arabic.* Notes Bull. Korean Chem. Soc., 2008. **29**(6): p. 1277.
79. Banerjee, S.S. and D.-H. Chen, *Magnetic nanoparticles grafted with cyclodextrin for hydrophobic drug delivery.* Chem. Mater., 2007. **19**: p. 6345-6349.
80. Banerjee, S.S. and D.-H. Chen, *Cyclodextrin conjugated magnetic colloidal nanoparticles as a nanocarrier for targeted anticancer drug delivery.* Nanotechnology, 2008. **19**(265602).
81. Jayakrishnan, A. and K.K. Nishi, *Self-gelling primaquine-Gum Arabic conjugate: an injectable controlled delivery system for primaquine.* Biomacromolecules, 2007. **8**: p. 84-90.
82. Jayakrishnan, A., K.K. Nishi, and M. Antony, *Synthesis and evaluation of ampicillin-conjugated gum arabic microspheres for sustained release.* Journal of pharmacy and pharmacology, 2007. **59**(4): p. 485-493.
83. Zhu, M.-T., et al., *Comparative study of pulmonary responses to nano- and submicron-sized ferric oxide in rats.* Toxicology, 2008. **247**: p. 102-111.
84. Motte, L., et al., *Bis-phosphonates - ultra small superparamagnetic iron oxide nanoparticles: a platform towards diagnosis and therapy.* Chem. Commun., 2008: p. 2553-2555.
85. Gupta, A.K. and A.S.G. Curtis, *Lactoferrin and ceruloplasmin derivatized superparamagnetic iron oxide nanoparticles for targeting cell surface receptors.* Biomaterials, 2004. **25**(24): p. 3029-3040.
86. Wilhelm, C. and F. Gazeau, *Universal cell labeling with anionic magnetic nanoparticles.* Biomaterials, 2008. **29**: p. 3161-3174.

87. Häfeli, U.O. and G.J. Pauer, *In vitro and in vivo toxicity of magnetic microspheres.* Journal of magnetism and magnetic materials, 1999. **194**: p. 76-82.
88. Park, J., et al., *In vitro effects of iron oxide nanoparticles in human monocytic cells.* Abstracts/Toxicology Letters, 2007. **172S**: p. I27.
89. Yiu, H.H.P., et al., *A triple-layer design for polyethyleneimine-coated nanostructured magnetic particles and their use in DNA binding and transfection.* Nanotechnology, 2007. **18**: p. 435601 (6 pp.).
90. Berry, C.C., et al., *The influence of transferrin stabilized magnetic nanoparticles on human dermal fibroblasts.* International Journal of Pharmaceutics, 2004. **269**: p. 211-225.
91. Yang, H. and X. Teng, *Effects of surfactants and synthetic conditions on the sizes and self-assembly of monodisperse iron oxide nanoparticles.* Journal of Materials Chemistry, 2004. **14**: p. 774-779.
92. Guin, D., et al., *One-pot size and shape controlled synthesis of DMSO capped iron oxide nanoparticles.* Bulletin of Materials Science, 2006. **29**(6): p. 617-621.
93. Williams, D.N., *Surface-modified magnetic nanoparticles for cellular interactions and improved biological applications*, in *Department of Chemical Engineering*. 2004, University of Maryland. p. 101.
94. Ma, H., et al., *Preparation and characterization of superparamagnetic iron oxide nanoparticles stabilized by alginate.* Pharmaceutical Nanotechnology, International Journal of Pharmaceutics, 2007. **333**: p. 177-186.
95. Iida, H., et al., *Synthesis of Fe3O4 nanoparticles with various sizes and magnetic properties by controlled hydrolysis.* Journal of Colloid and Interface Science, 2007. **314**: p. 274 - 280.
96. Doelsch, E., et al., *Crystal Chemistry of Colloids Obtained by Hydrolysis of Fe(III) in the Presence of SiO4 Ligands.* Mat. Res. Soc. Symp. Proc., 2001: p. 658.
97. Groman, E.V., et al., *Delivery of therapeutic agents to receptors using polysaccharides*. 1996: United States Patent.
98. Nothnagel, E.A., et al., *Chemical investigation of the structural basis of the emulsifying activity of gum arabic.* Food Hydrocolloids, 2007. **21**: p. 297-308.
99. Kaiser, E., et al., *Color test for detection of free terminal amino groups in solid-phase synthesis of peptides.* Anal. Biochem, 1970. **34**: p. 595-598.

100. Fluka, K.T.
101. Bicinchoninic Acid Protein Assay Kit - Technical Bulletin, S.
102. Cardoso, A.S., *Magnetic nanoparticle functionalization with bipolymers*, in *Department of Chemistry*. 2007, Faculdade de Ciências e Tecnologia - UNL: Lisbon.
103. Freshney, R.I., *Culture of animal cells: A manual of basic technique*. Third edition ed. 1994: John Wiley and Sons, Inc. xxiv+486p.
104. Invitrogen, *Viable Cell Counts Using Trypan Blue*.